Freezing of Soil and Geomorphology

Alan Rempel

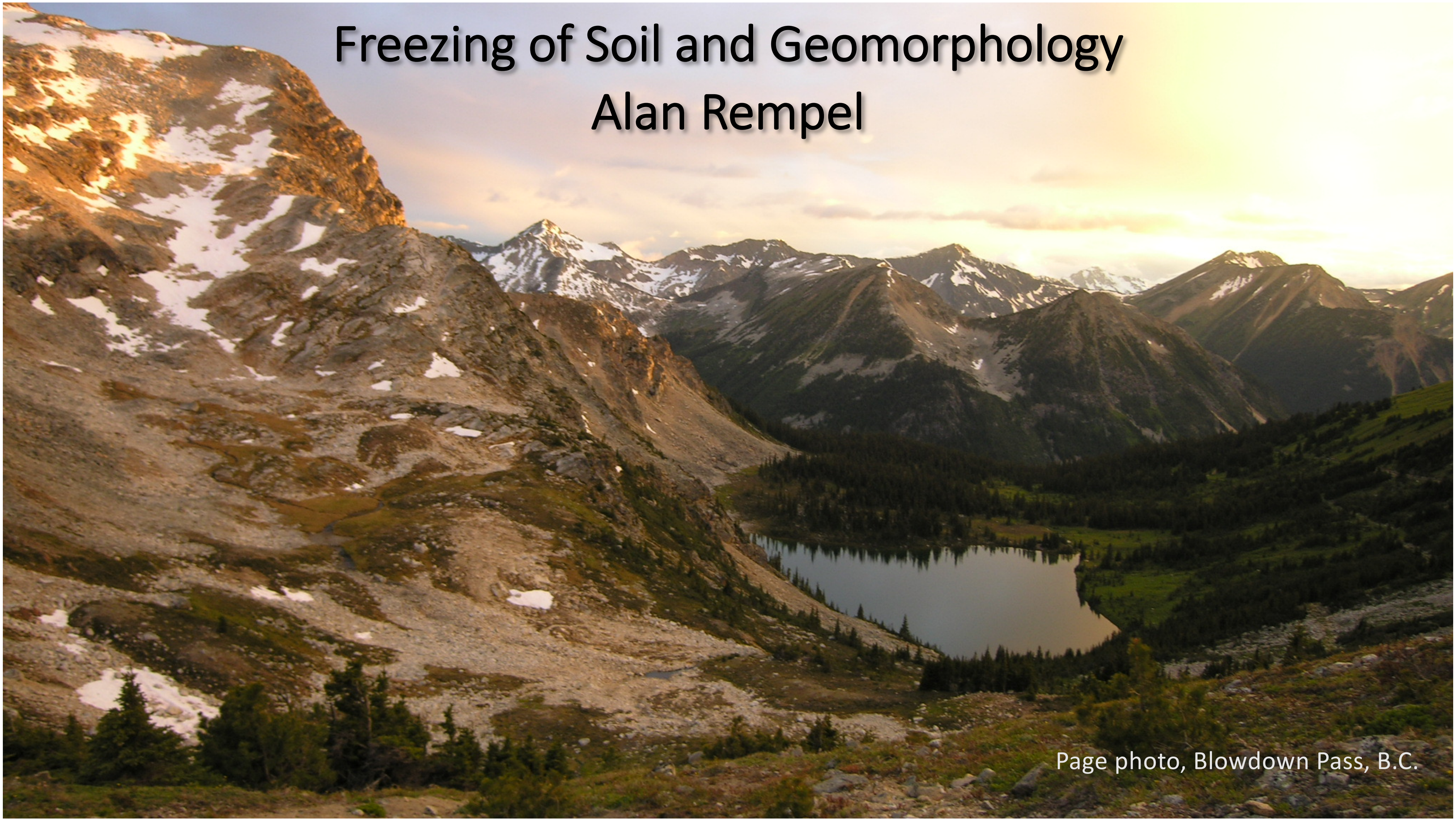

Page photo, Blowdown Pass, B.C.

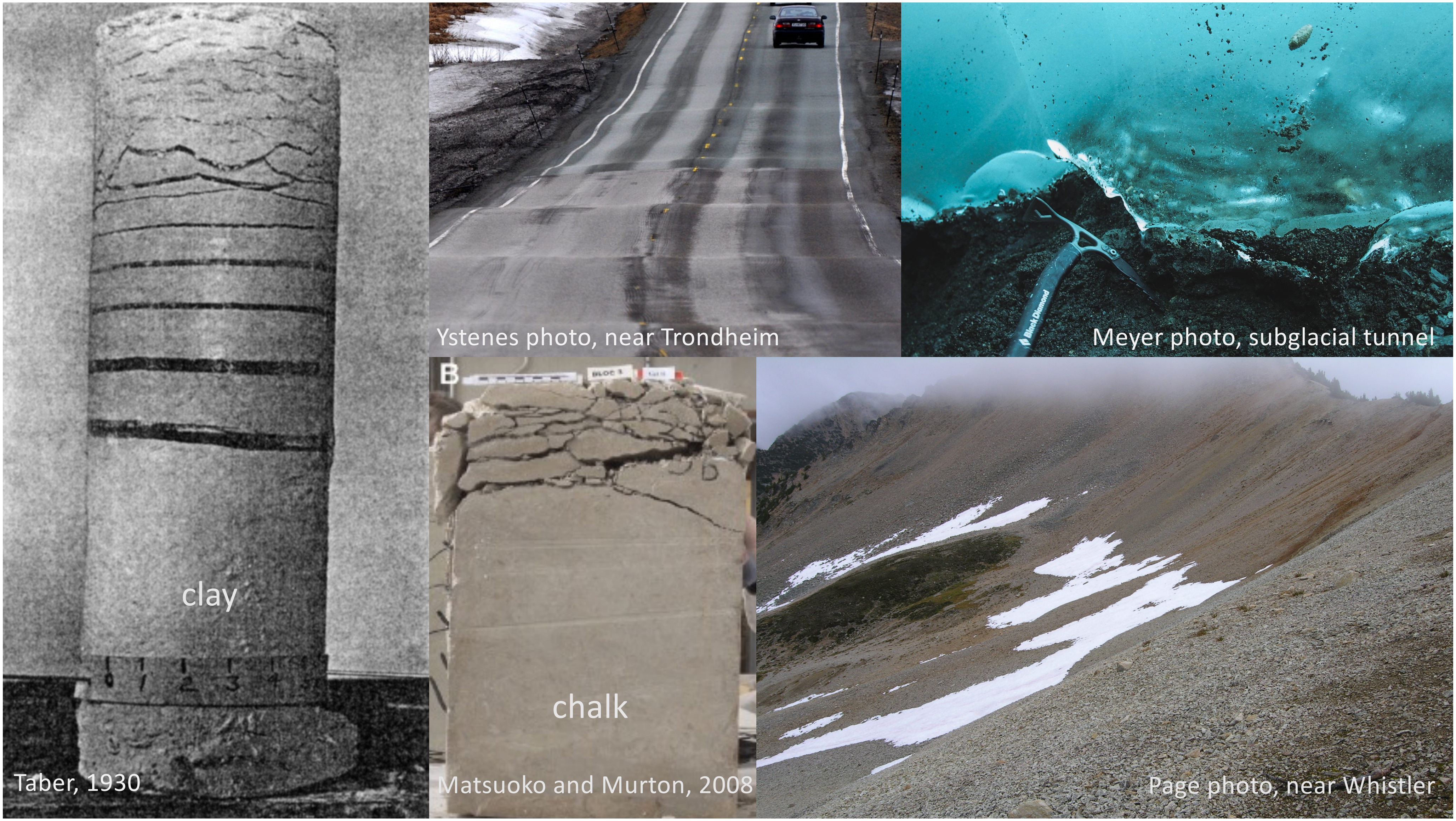
Ystenes photo, near Trondheim
Meyer photo, subglacial tunnel
clay
Taber, 1930
B
chalk
Matsuoko and Murton, 2008
Page photo, near Whistler

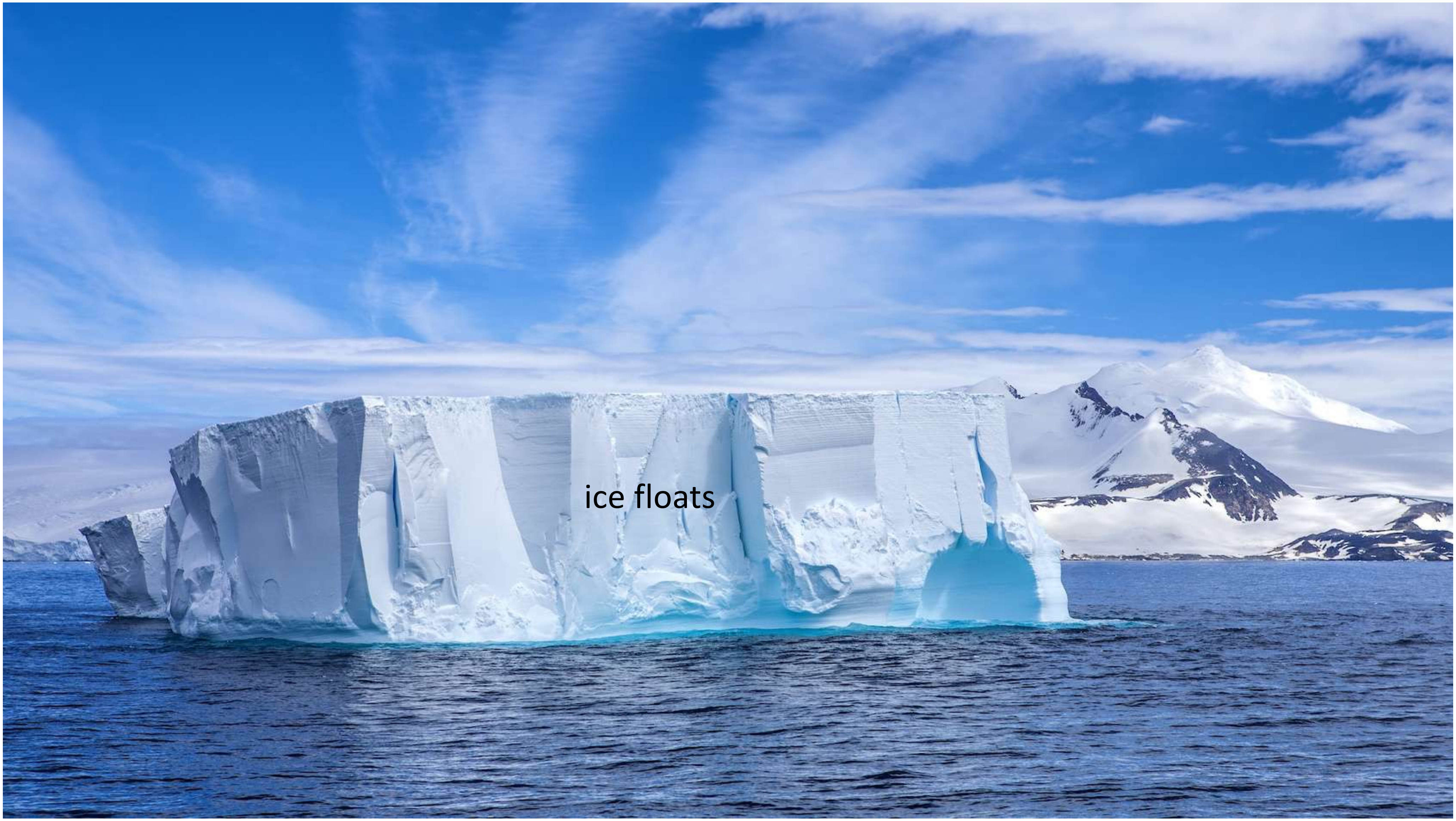
ice floats

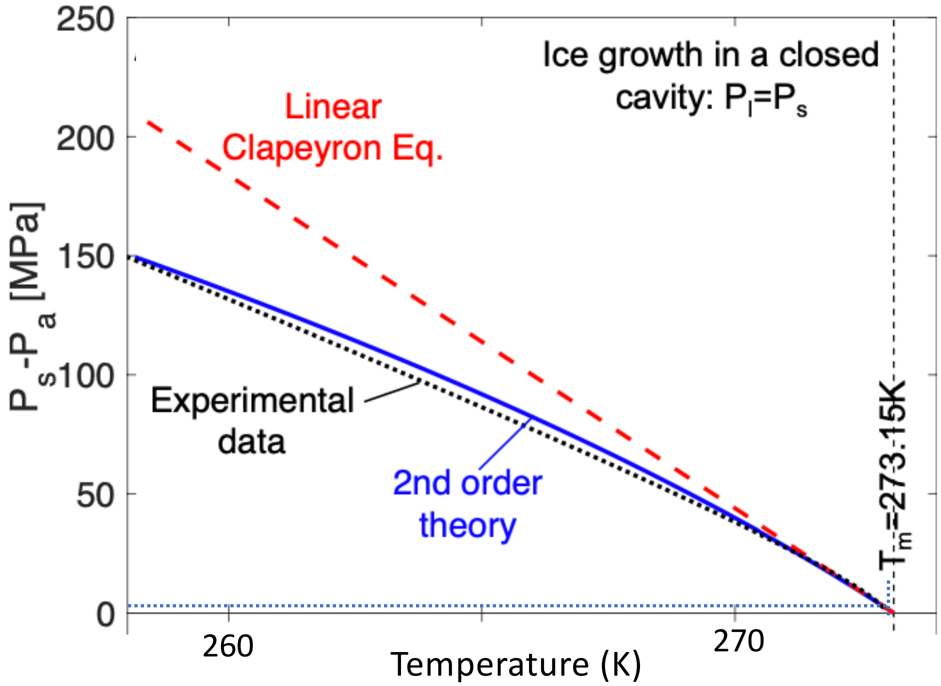

A disastrous consequence of the increase in density upon freezing.

What freezer temperature would have been safe?

Estimated tensile strength: 6 MPa

Clapeyron slope: $\frac{dT}{dP} \approx 0.73\,\frac{\mathrm{K}}{\mathrm{MPa}}$

In closed system expected: $\Delta T \approx -0.43\ \mathrm{K}$

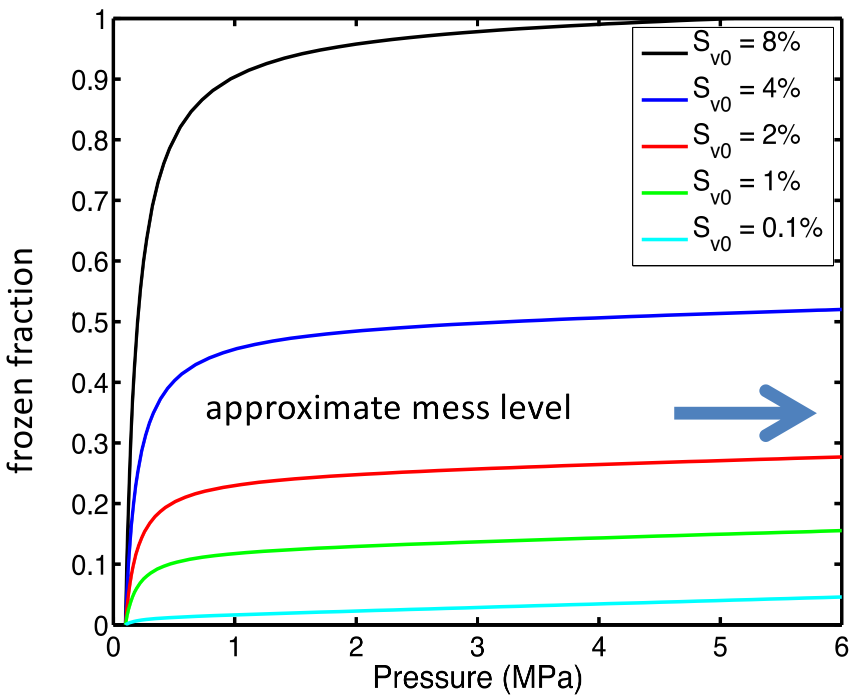

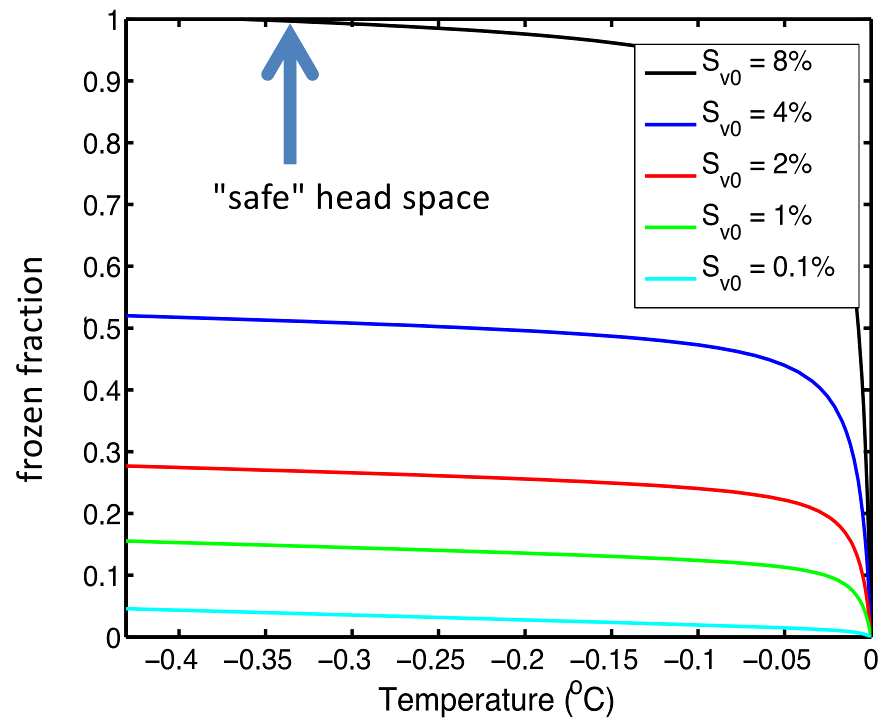

- conservation of beer plus ice
- conservation of vapor (probably wrong)
- linear liquid/ice compressibilities
- neglect freezing point depression from alcohol
- rapid fluid and heat redistribution
- P_0= 10^5 Pa, vapor volume fraction S_{v0}

When >91% of the pores of concrete are filled with water... [and] ... these molecules freeze, they expand by 9%, and because there is no room for their increased volume, the concrete distresses. The freeze can cause the bonds in cement around the aggregate to break ... As the seasons pass, concrete goes through the process of freezing and thawing, wearing out over time.

Images and text from civildigital.com

2007 Monthly freeze/thaw time series

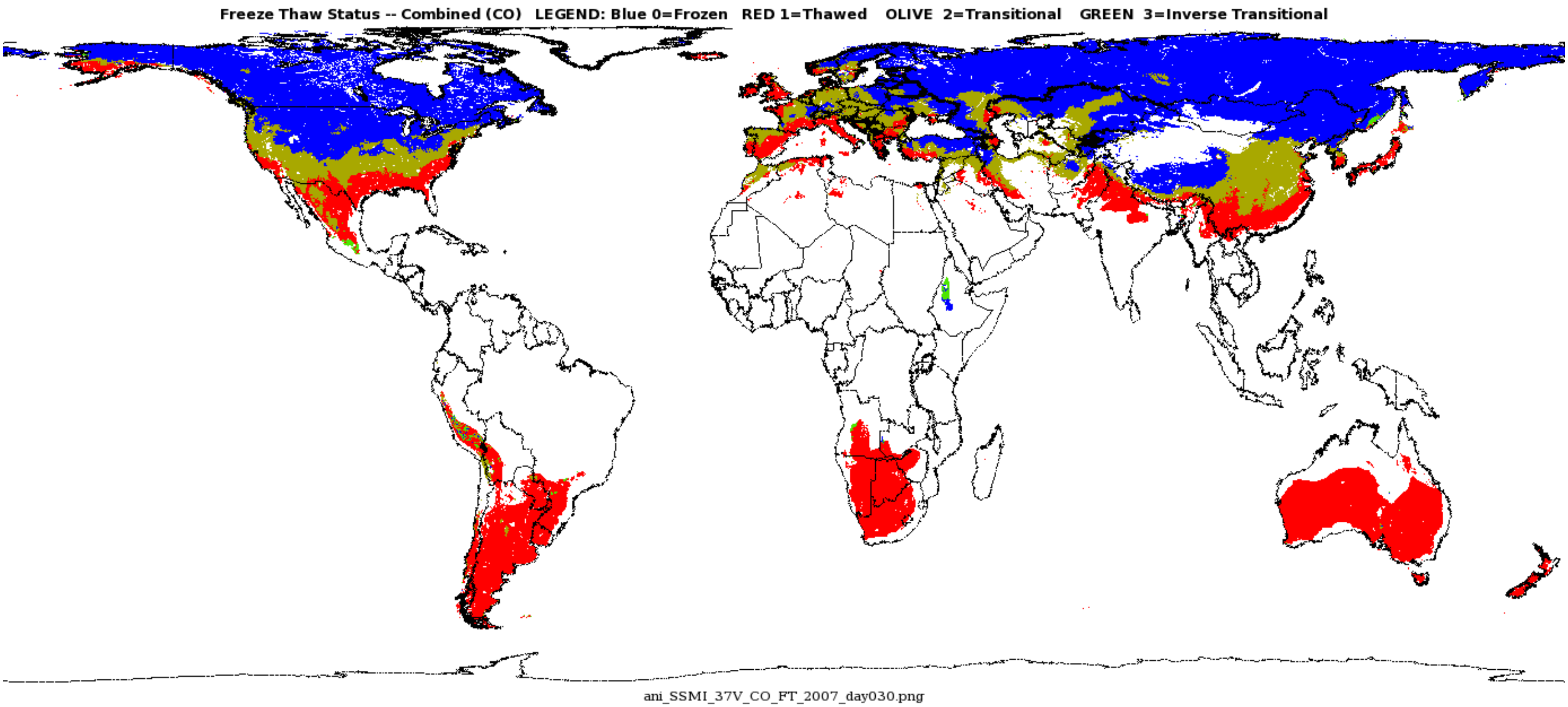

downloaded from: https://www.umt.edu/numerical-terradynamic-simulation-group/freeze-thaw/

Mechanisms:

1. volumetric expansion (should occur near 0°C, favored by low S_{v0})

2. thermal expansion cracking (more prominent with rapid T change, no direct dependence on S_{v0})

3. segregated ice growth
(liquid flow towards freezing sites, requires T cold enough to propagate cracks)

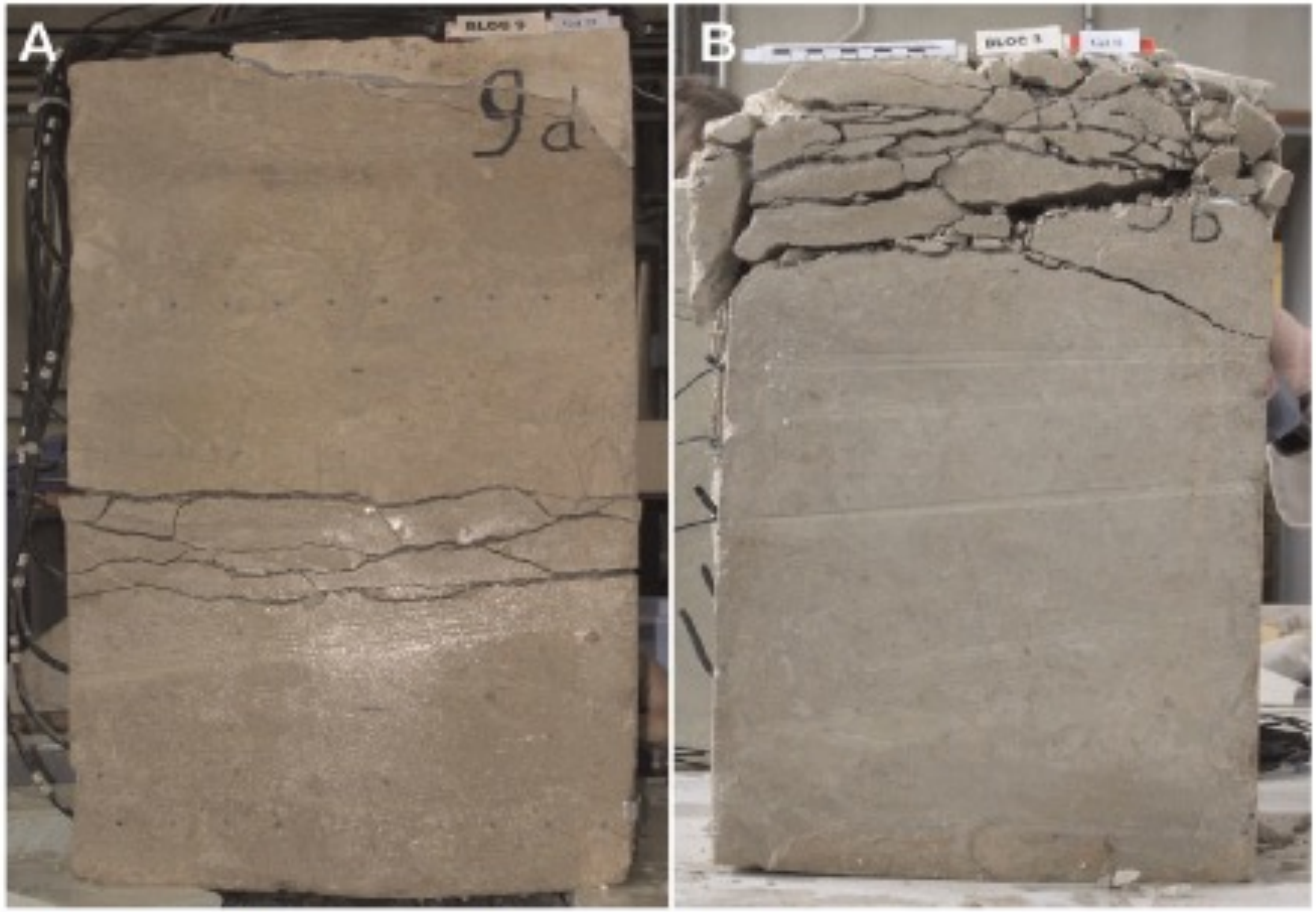

Matsuoka and Murton, 2008

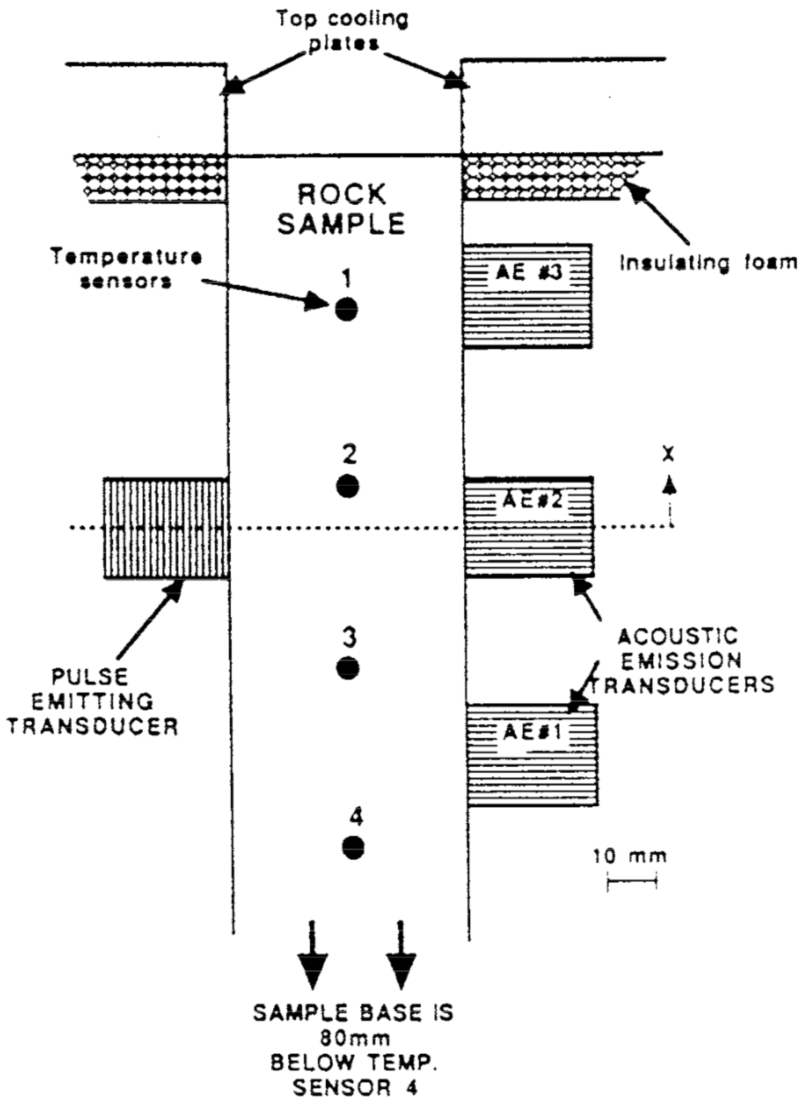

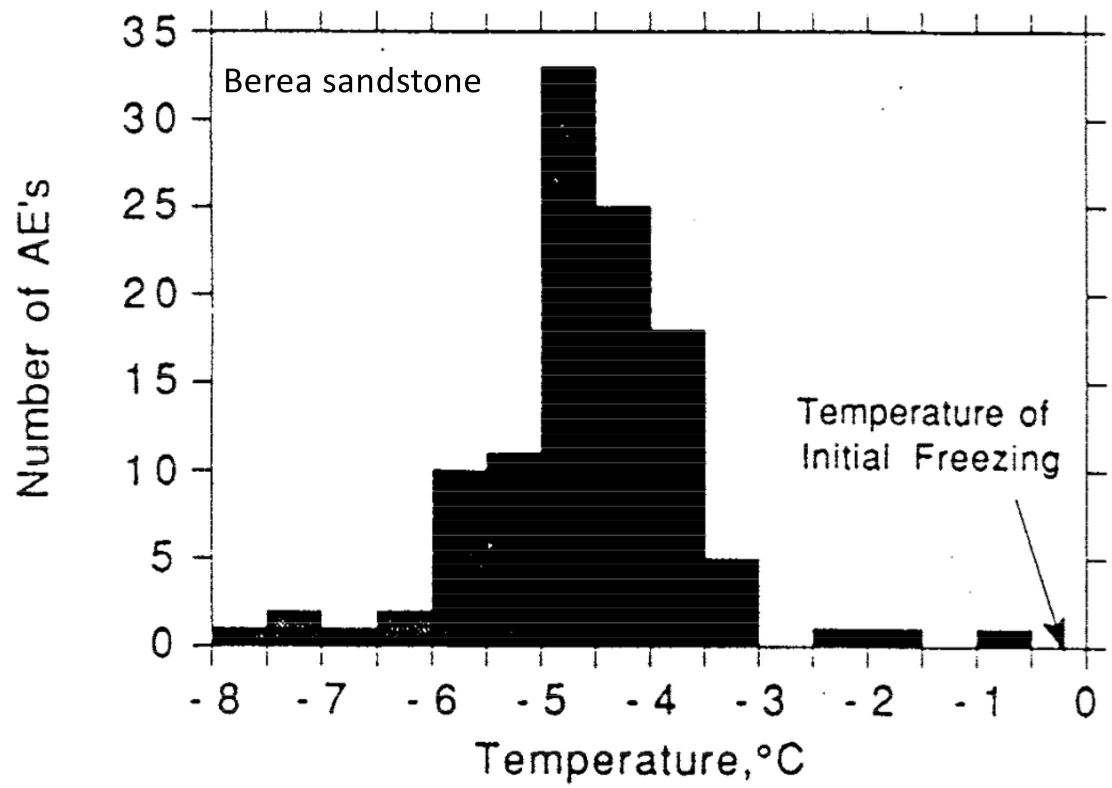

Hallet et al., 1991

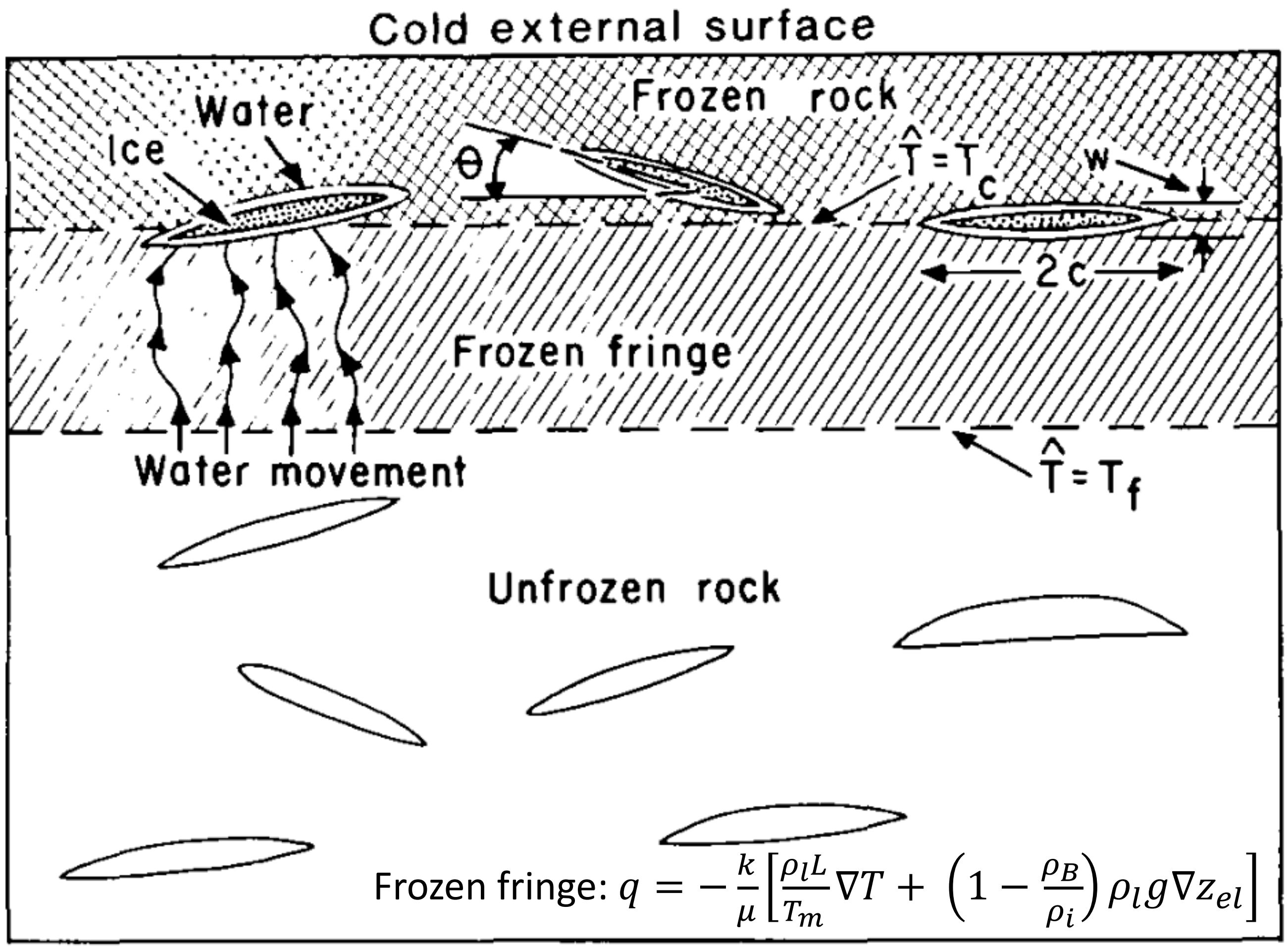

Frozen fringe: $q = -\frac{k}{\mu}\left[\frac{\rho_l L}{T_m}\nabla T + \left(1 - \frac{\rho_B}{\rho_i}\right)\rho_l g \nabla z_{el}\right]$

Walder and Hallet, 1985

- stress intensity factor
  $$K_I = \lim_{r \to 0} \sqrt{2\pi r}\,\sigma_{yy}(r, 0)$$
- penny-shaped crack:
  $$K_I = \sqrt{\frac{4c}{\pi}} P_i$$
- subcritical crack growth once K_I exceeds a "stress corrosion limit"
- extension rate determined by mass balance (partly by corrosion kinetics, and partly by water transport)

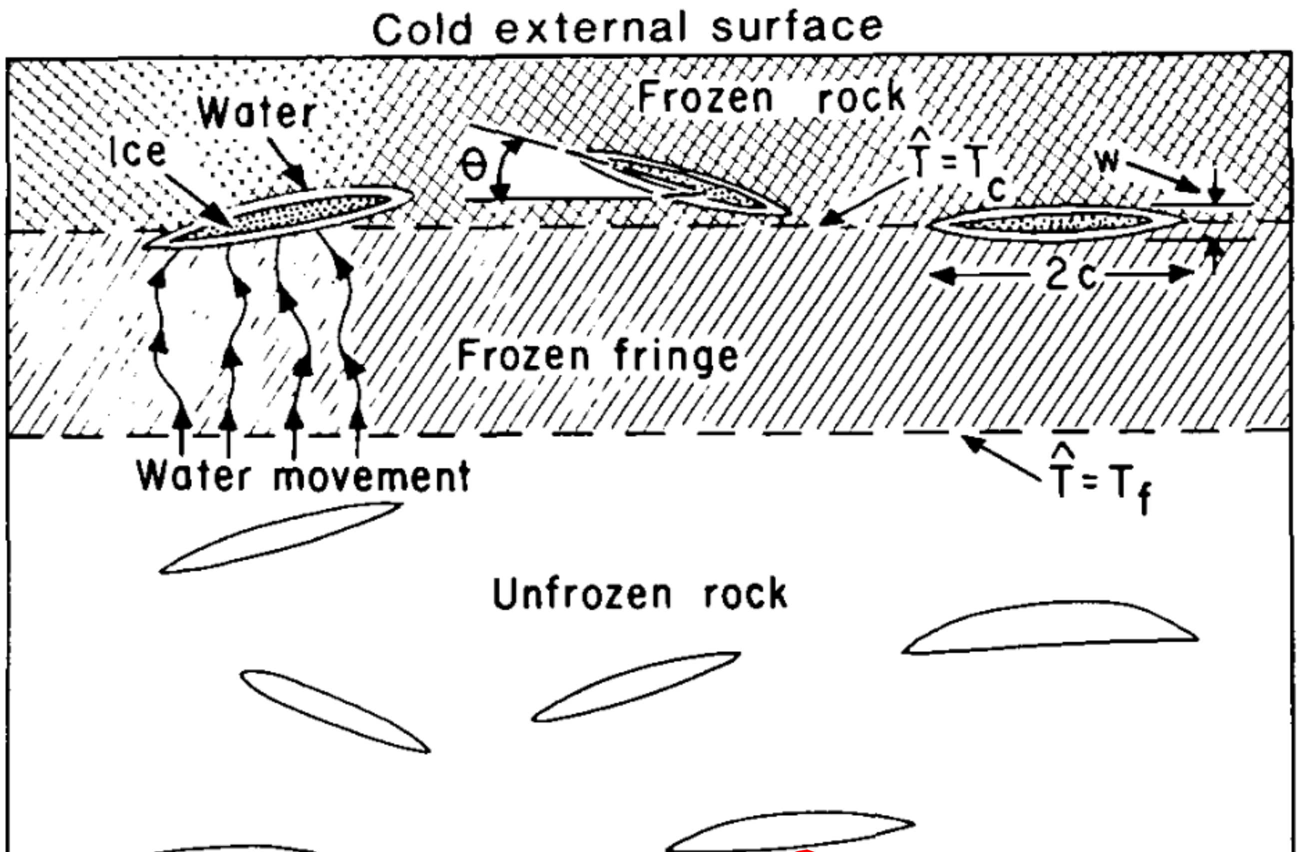

Frozen fringe: $q = -\frac{k}{\mu}\left[\frac{\rho_l L}{T_m}\nabla T + \left(1 - \frac{\rho_B}{\rho_i}\right)\rho_l g \nabla z_{el}\right]$

aka "crystallization pressure"
~1.2 MPa/K (1.1 MPa/K if ρ_i used)

Walder and Hallet, 1985

- stress intensity factor
  $$K_I = \lim_{r \to 0} \sqrt{2\pi r}\sigma_{yy}(r, 0)$$
- penny-shaped crack:
  $$K_I = \sqrt{\frac{4c}{\pi}} P_i$$
- subcritical crack growth once K_I exceeds a "stress corrosion limit"
- extension rate determined by mass balance (partly by corrosion kinetics, and partly by water transport)

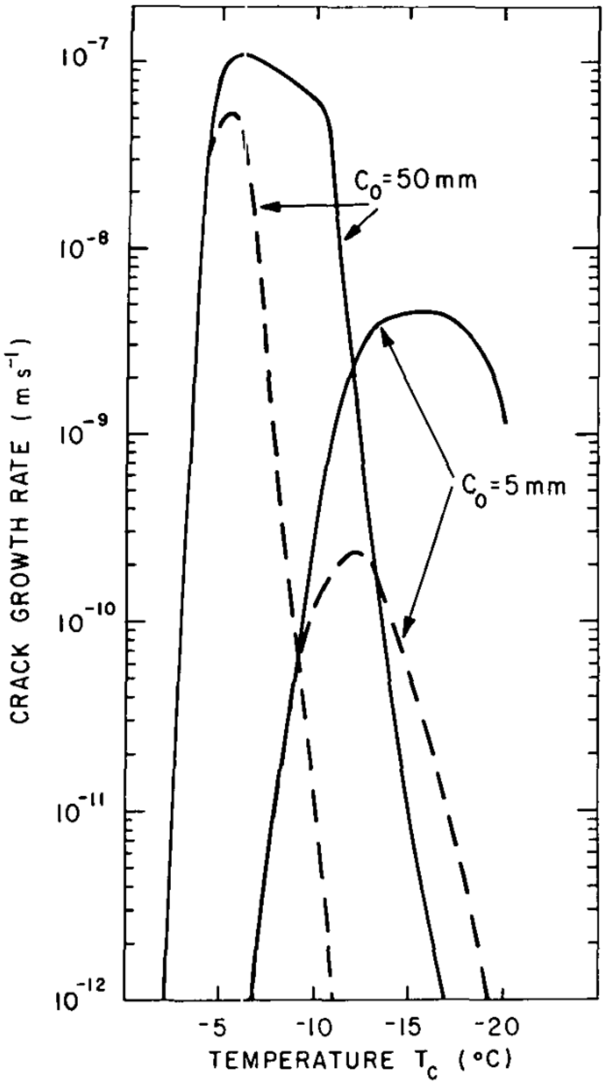

subcritical crack growth:

Westerly Granite,
∇T =0.1 °C/mm

Fastest crack growth:

- biggest cracks
- intermediate T

dashed: freezing for 50 hours
solid: freezing for 100 hours

dashed: initial crack radius 5mm
solid: initial crack radius 50mm

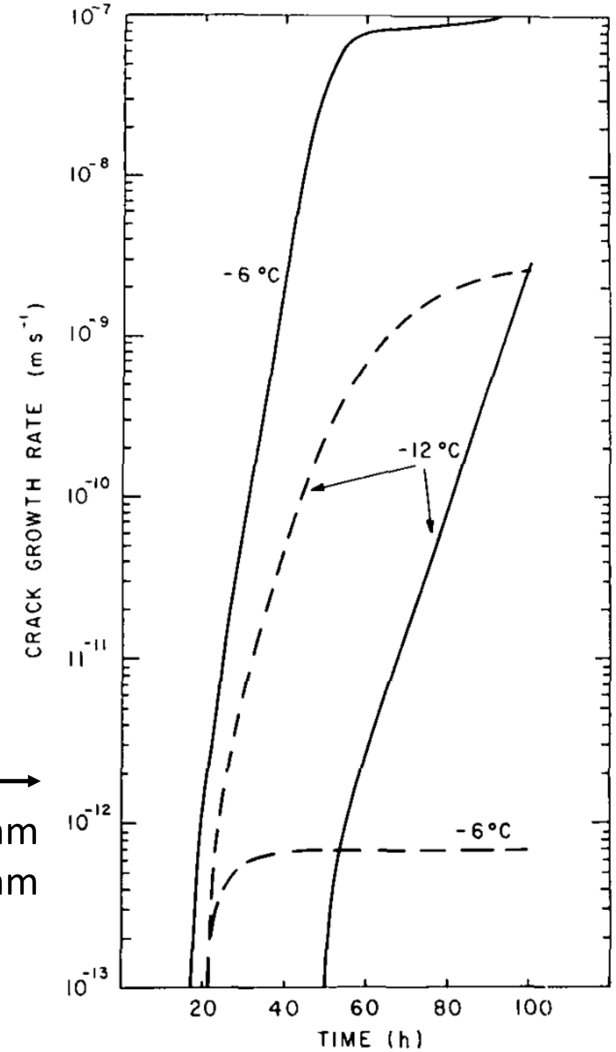

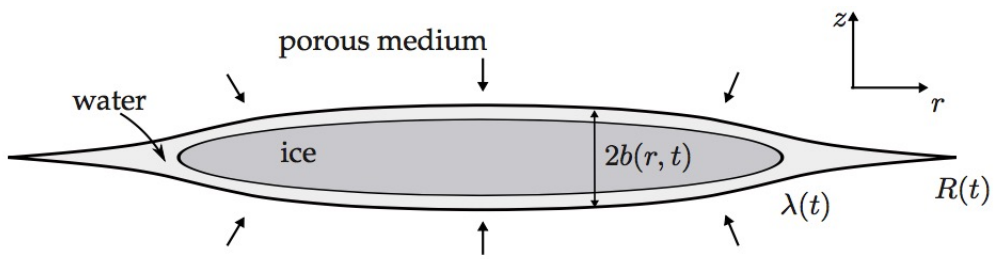

Assume crack growth at critical stress intensity factor.

Small cracks deform elastically; extension of larger cracks limited by water supply.

too warm to crack

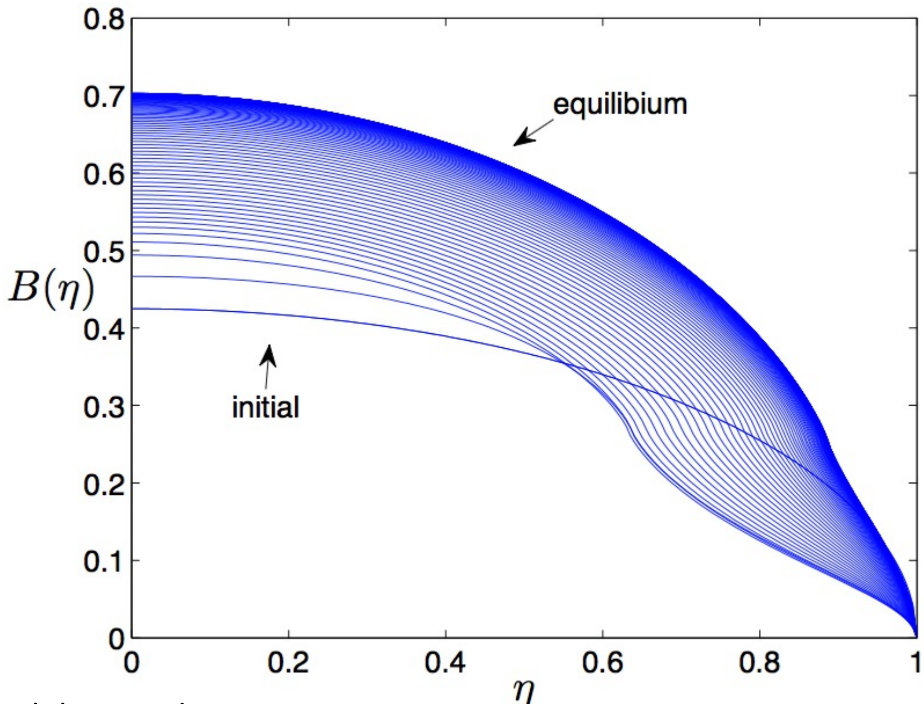

Vlahou and Worster, 2015

crack growth in limestone at -10 ^{o}C

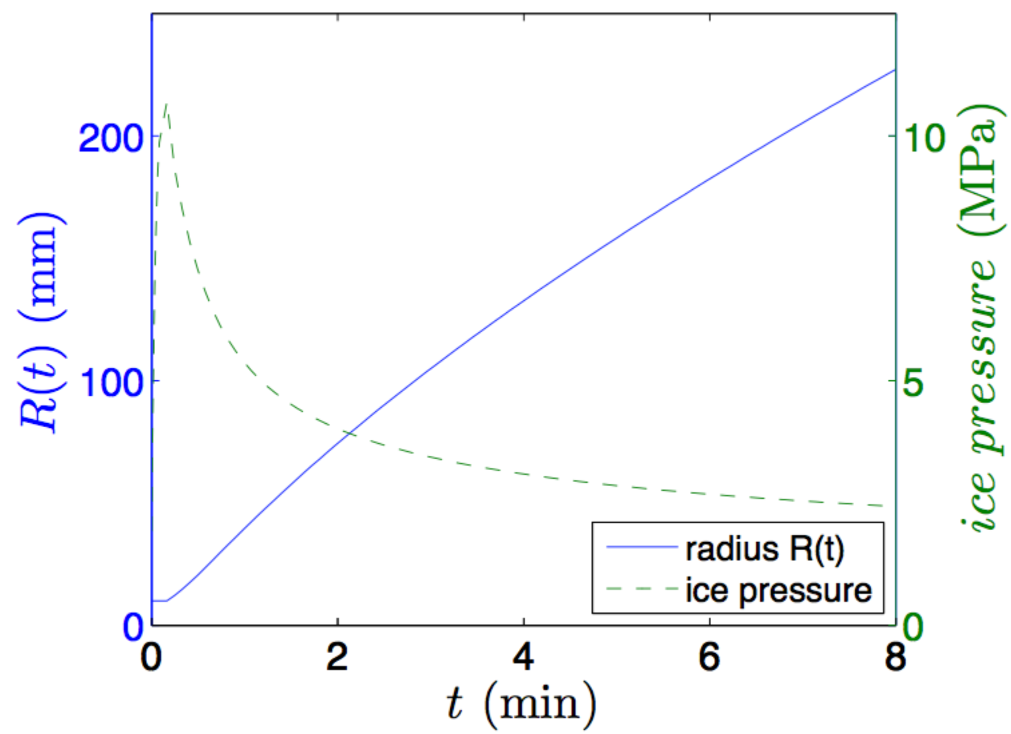


Some upscaling may be necessary.

Hales and Roering, 2007

Tracking the behavior of each crack is not feasible.

A cracking index to gauge likely damage may help.

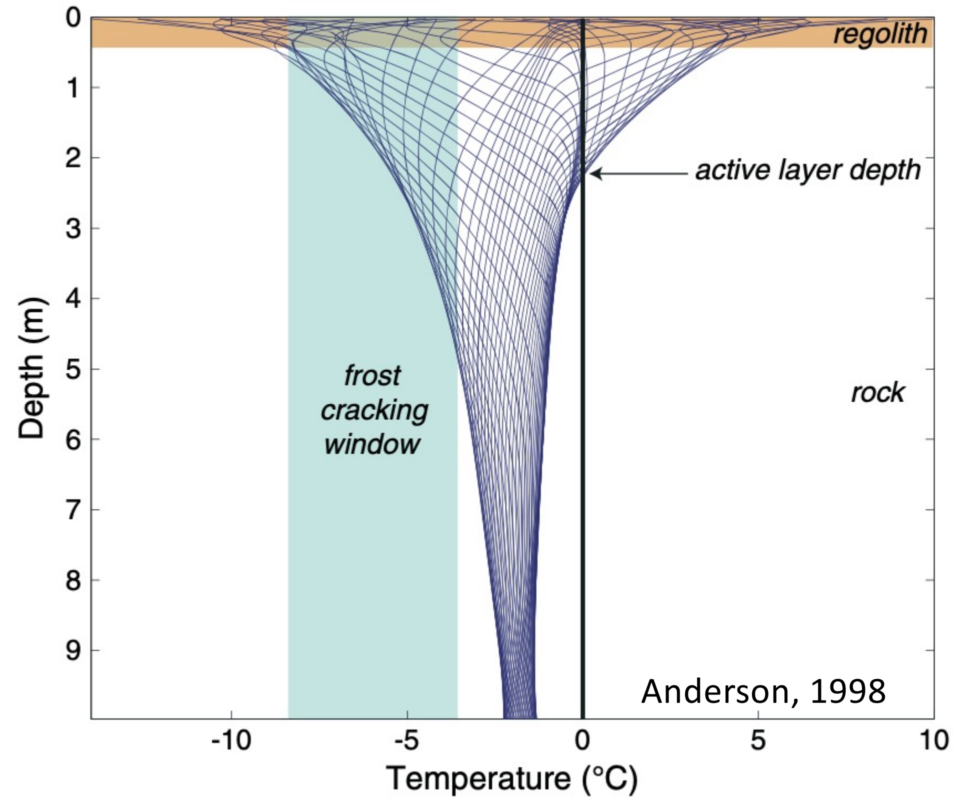

$$T(z,t) = MAT - A\exp\left(-z\sqrt{\frac{\pi}{\kappa P_y}}\right)\cos\left(\frac{2\pi t}{P_y} - z\sqrt{\frac{\pi}{\kappa P_y}}\right)$$

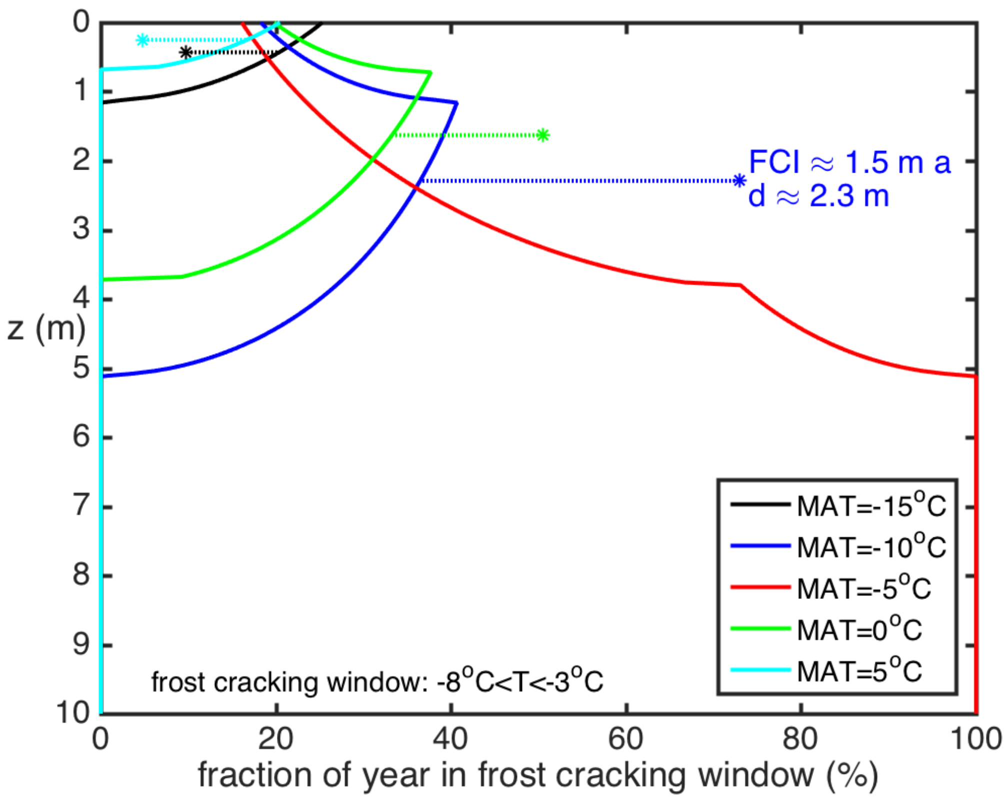

Index 1: damage increases in proportion to time within a "frost cracking window"

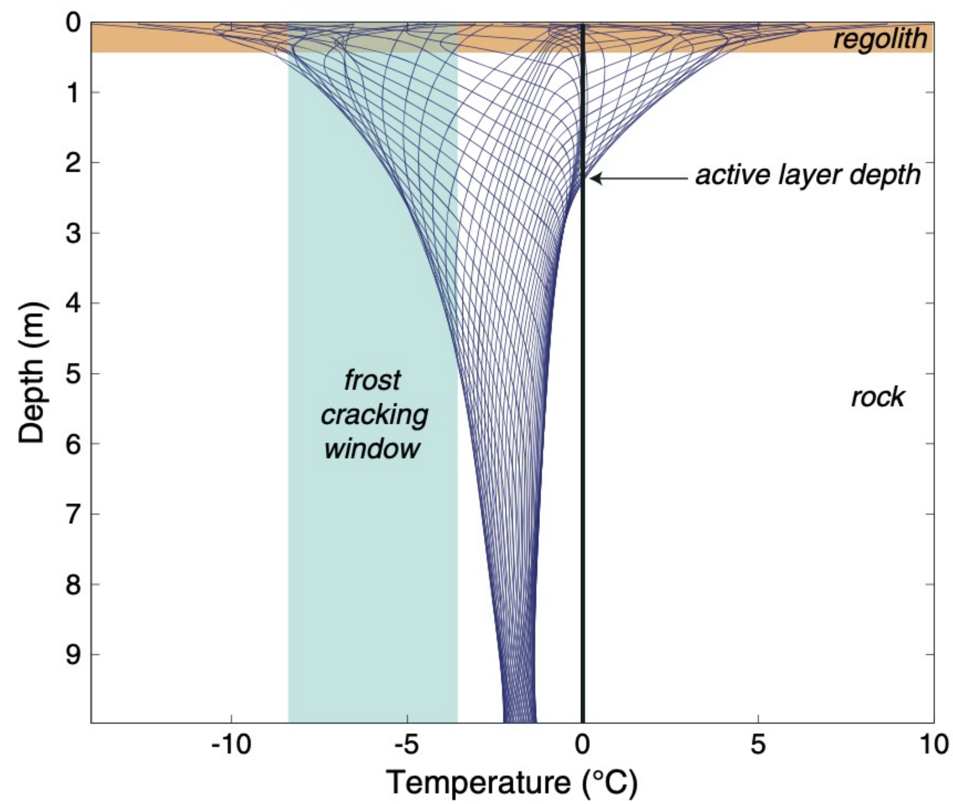

$$T(z,t) = MAT - A\exp\left(-z\sqrt{\frac{\pi}{\kappa P_y}}\right)\cos\left(\frac{2\pi t}{P_y} - z\sqrt{\frac{\pi}{\kappa P_y}}\right)$$

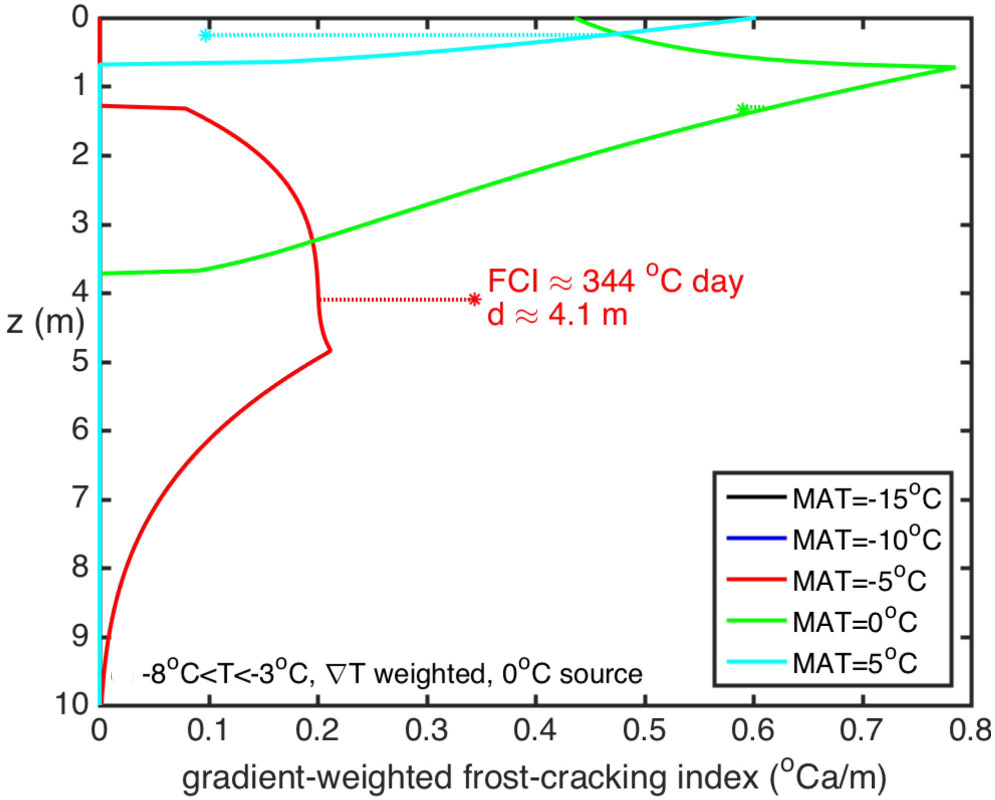

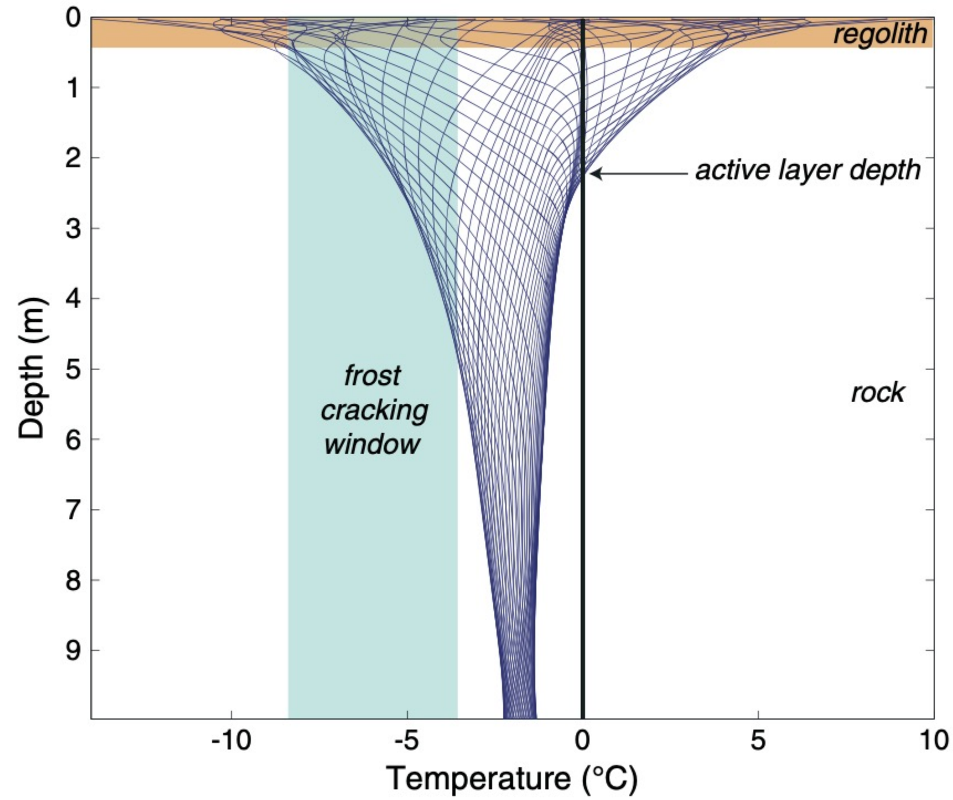

Index 2: damage increases in proportion to time and T gradient within "fcw'

$$T(z,t) = MAT - A\exp\left(-z\sqrt{\frac{\pi}{\kappa P_y}}\right)\cos\left(\frac{2\pi t}{P_y} - z\sqrt{\frac{\pi}{\kappa P_y}}\right)$$

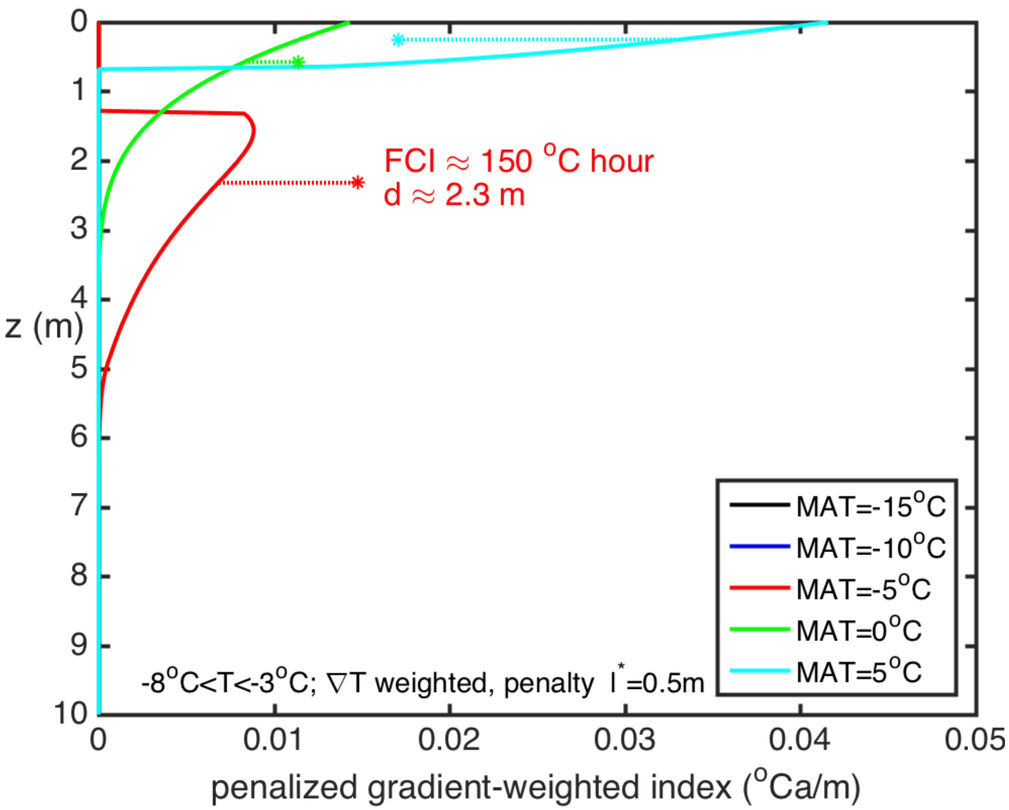

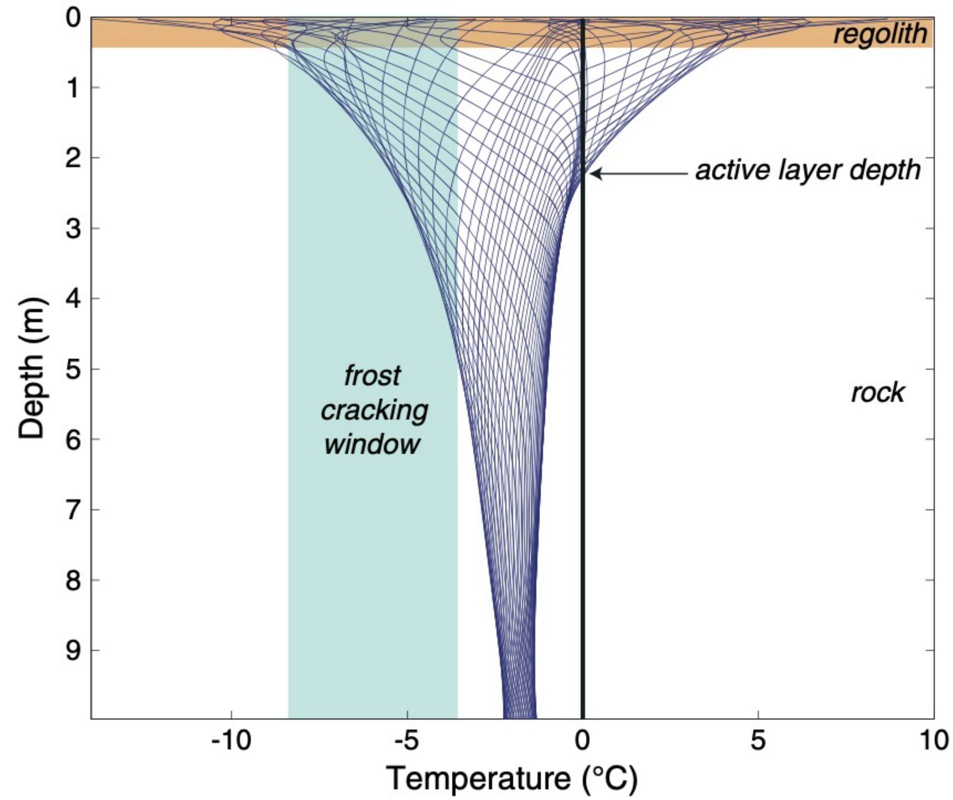

Index 3: damage increases in proportion to time and ∇T within "fcw", if free water

$$T(z,t) = MAT - A\exp\left(-z\sqrt{\frac{\pi}{\kappa P_y}}\right)\cos\left(\frac{2\pi t}{P_y} - z\sqrt{\frac{\pi}{\kappa P_y}}\right)$$

Tracking the behavior of each crack is not feasible.

A cracking index to gauge likely damage may help.

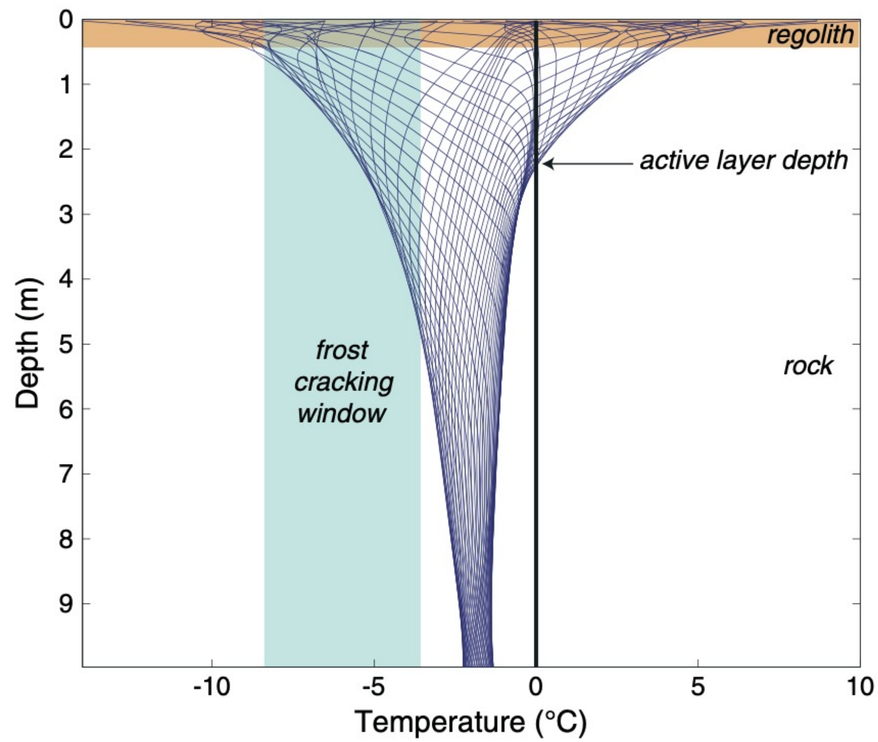

How does frost damage depend upon environmental factors and material properties over relevant scales in length and time?

Suppose frost damage correlates with ice growth that extends cracks.
How does porosity change when it is cold enough to crack?

1. Assume cracking once $K_I = K_c$ so for a single characteristic crack shape, require: $P_i = P_c$

2. Mass balance ($S_l = 1$ initially) and Darcy's law with a temperature-dependent permeability:

$$\frac{\partial n}{\partial t} = \nabla \cdot \left(\frac{k}{\mu}\nabla P\right) = \mu^{-1}\left(\frac{\mathrm{d}k}{\mathrm{d}T}\nabla T \cdot \nabla P + k\nabla^2 P\right)$$

3. Generalized Clapeyron equation with $P_i = P_c$ implies $\nabla P = \frac{\rho L}{T_m}\nabla T$ so

$$\frac{\partial n}{\partial t} = \frac{\rho L}{T_m \mu}\left[\frac{\mathrm{d}k}{\mathrm{d}T}(\nabla T)^2 + k\nabla^2 T\right]$$

4. Ignore latent heat; assume cracking begins long after most water already frozen so $S_l \ll 1$

$$\frac{\partial n}{\partial t} \approx \frac{\rho L}{T_m \mu}\left[\frac{\mathrm{d}k}{\mathrm{d}T}(\nabla T)^2 + \frac{k}{\kappa}\frac{\partial T}{\partial t}\right]$$

5. Assume periodic annual thermal forcing

$$\Delta n(z, 1\mathrm{year}) = \frac{\rho L}{T_m \mu}\int_{\Delta T > \Delta T_c} \frac{\mathrm{d}k}{\mathrm{d}T}\left(\frac{\partial T}{\partial z}\right)^2 \mathrm{d}t$$

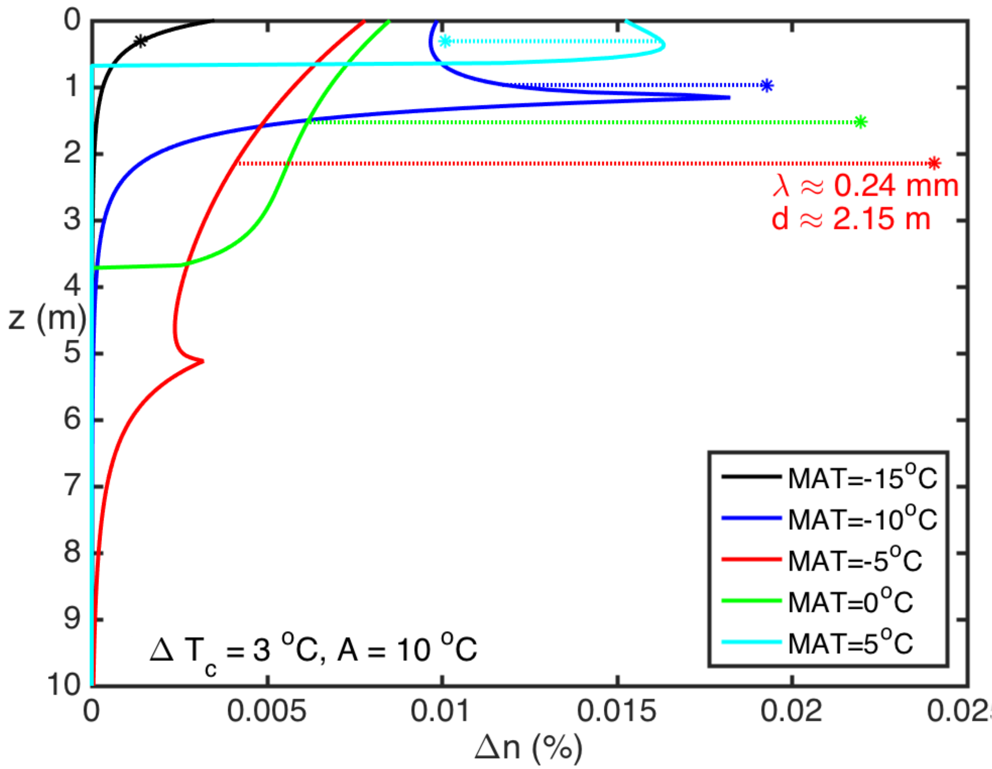

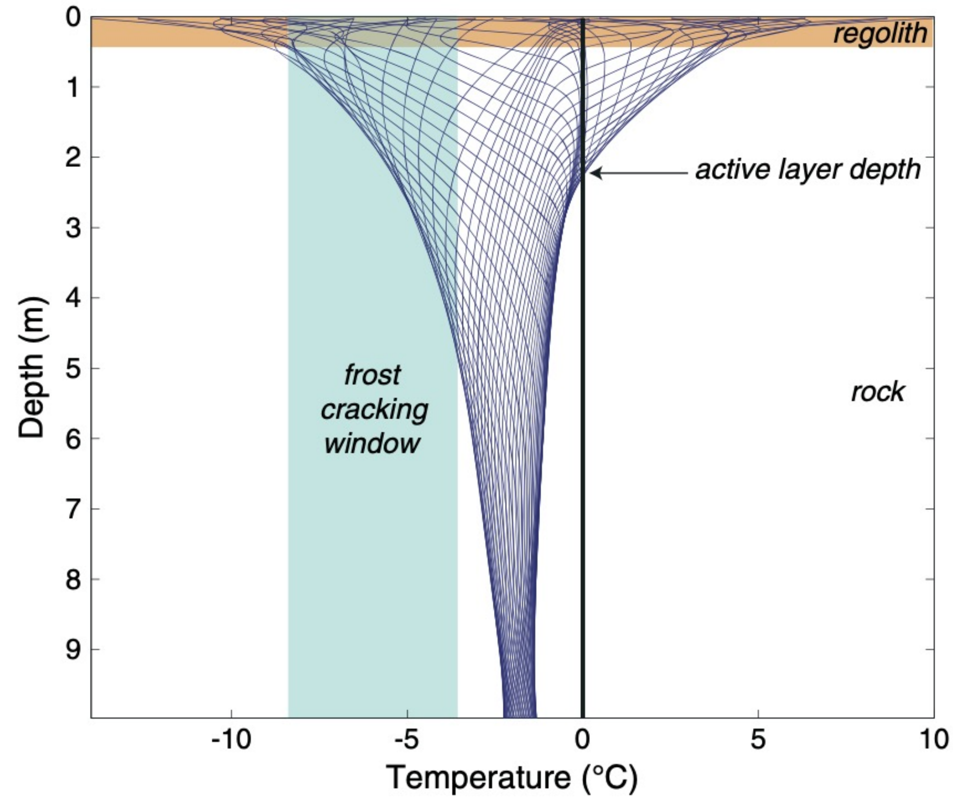

$$\Delta n(z) = \frac{D}{\Delta T_c^2} \int_{\Delta T > \Delta T_c, 1\ \text{year}} \left(\frac{\Delta T_c}{\Delta T}\right)^{\alpha+1} \left(\frac{\partial T}{\partial z}\right)^2 \mathrm{dt}$$

$$D = \alpha \rho L k_c \Delta T_c / (T_m \mu)$$

$$T(z,t) = MAT - A \exp\left(-z\sqrt{\frac{\pi}{\kappa P_y}}\right) \cos\left(\frac{2\pi t}{P_y} - z\sqrt{\frac{\pi}{\kappa P_y}}\right)$$

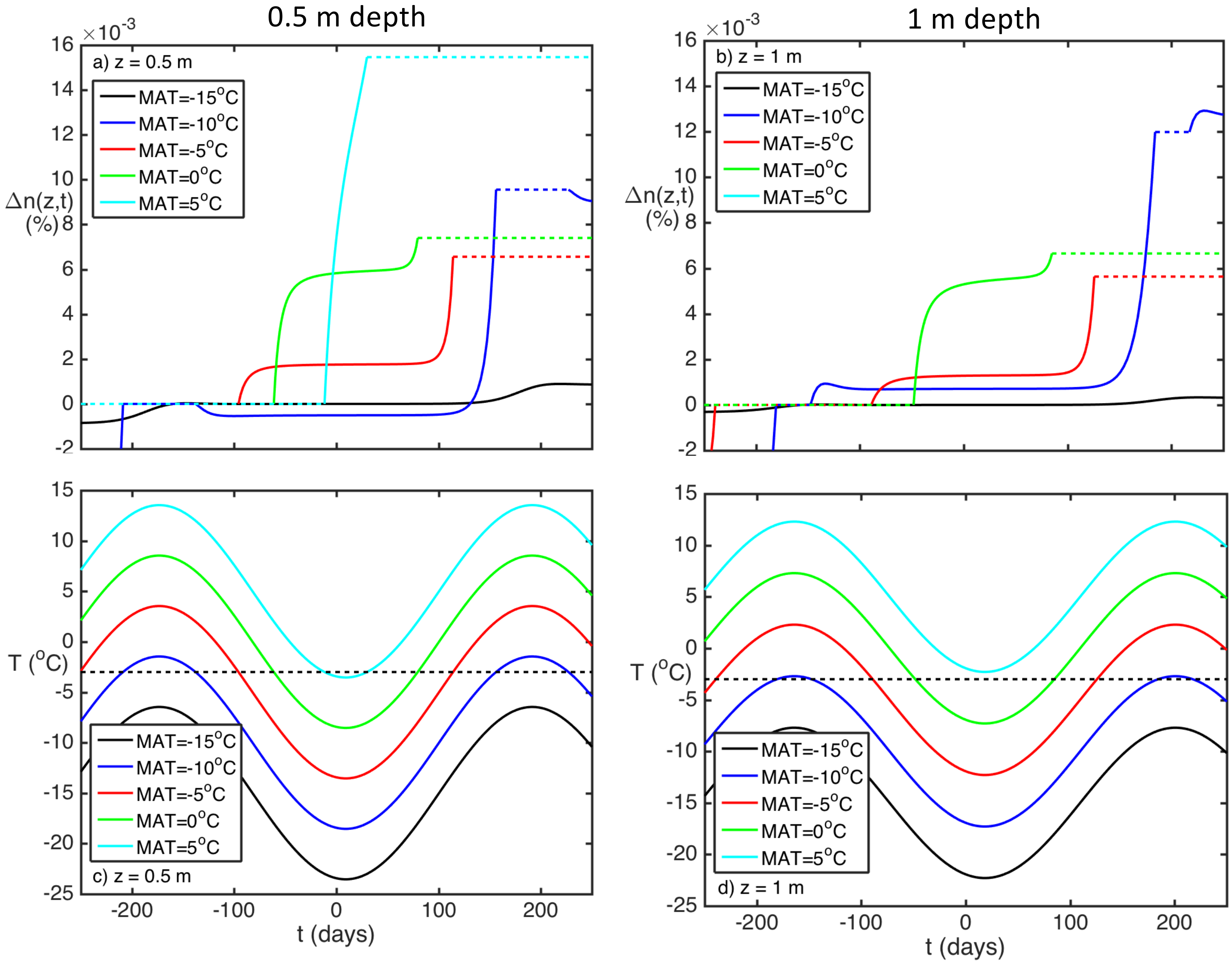

How does the timing of crack-driven porosity increases vary with climate?

$$\frac{\partial n}{\partial t} = \frac{\rho L}{T_m \mu}\left[\frac{\mathrm{d}k}{\mathrm{d}T}(\nabla T)^2 + k\nabla^2 T\right]$$

$$k = k_0\left(\frac{\Delta T_f}{\Delta T}\right)^{\alpha}$$

- only in winter if just cold enough
- most intense in fall if somewhat colder
- most intense in spring when still colder
- only in summer in coldest cases

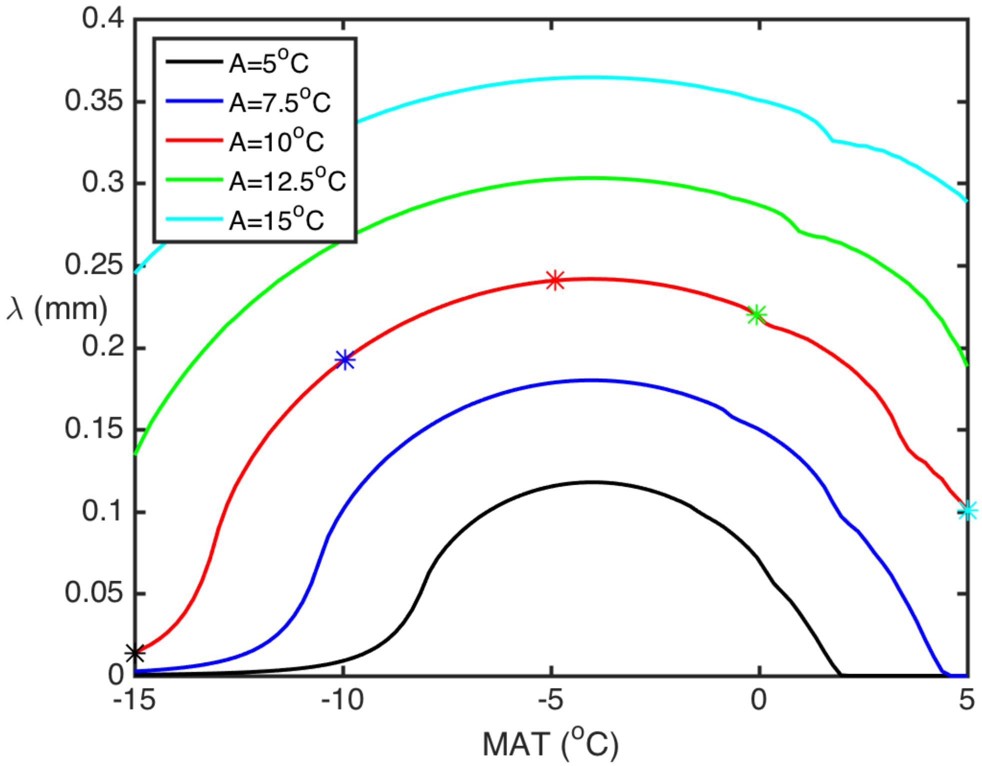

$$\lambda = \int_{\Delta T \geq \Delta T_c} \Delta n(z)\, \mathrm{d}z$$

Greatest depth-integrated deformation with largest seasonal amplitudes – especially if MAT close to crack growth onset temperatures.

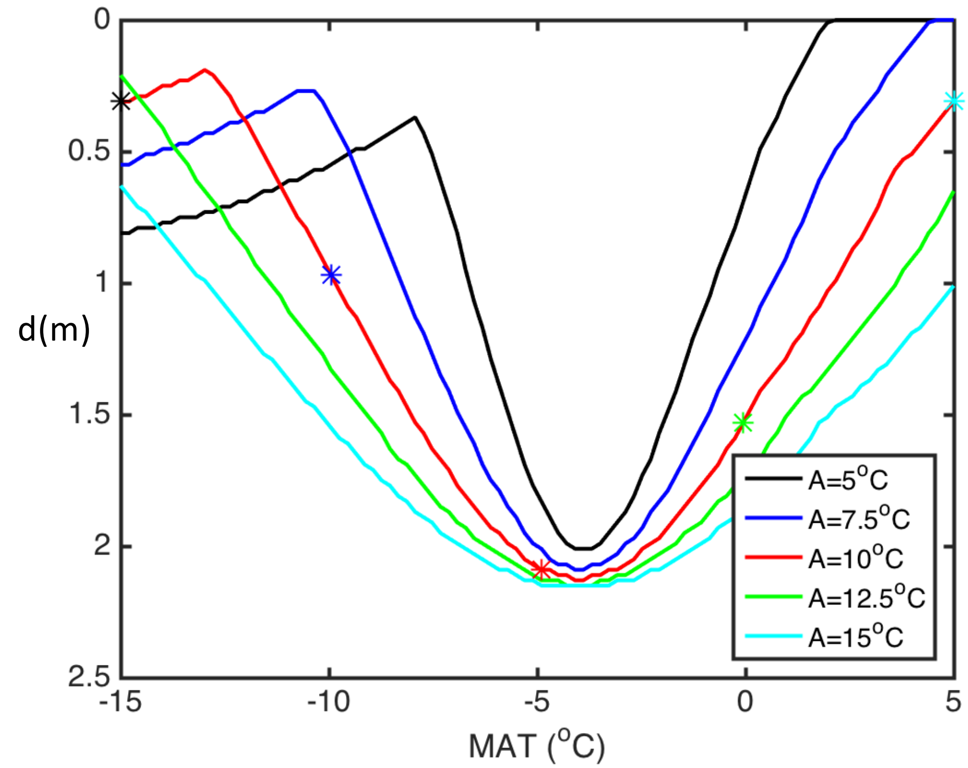

$$\int_0^d \Delta n(z)\mathrm{d}z = \lambda / 2$$

"Swell depth" gets deeper as MAT decreases, but shallows once again when MAT below crack onset temperature.

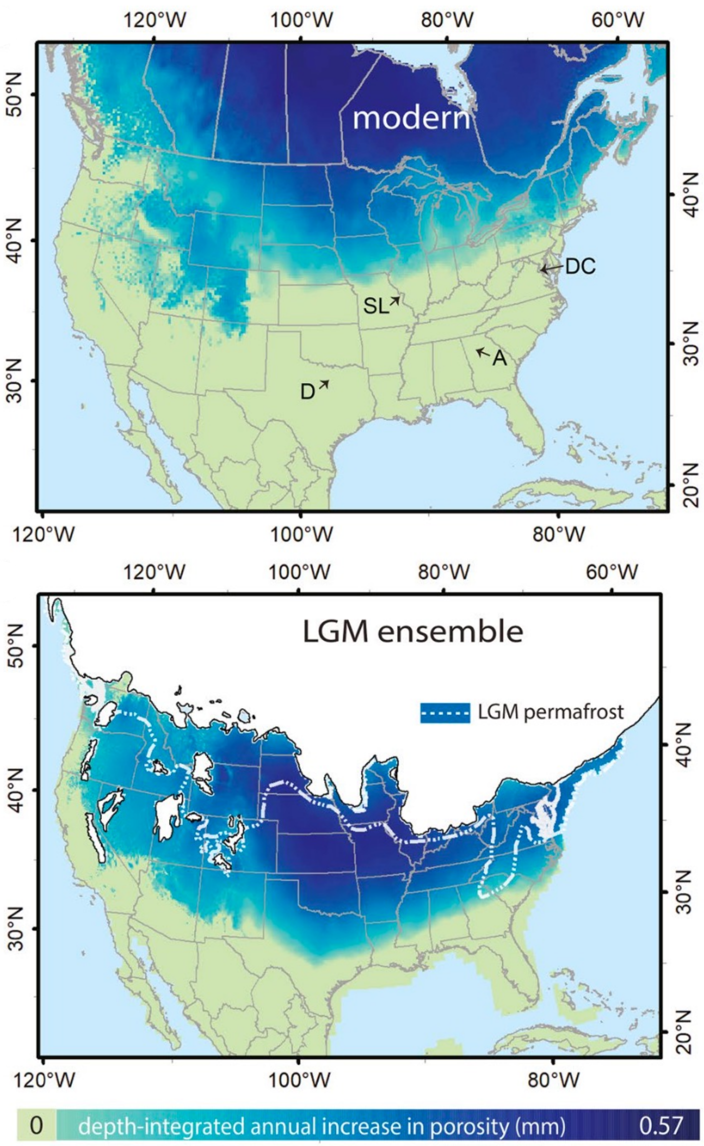

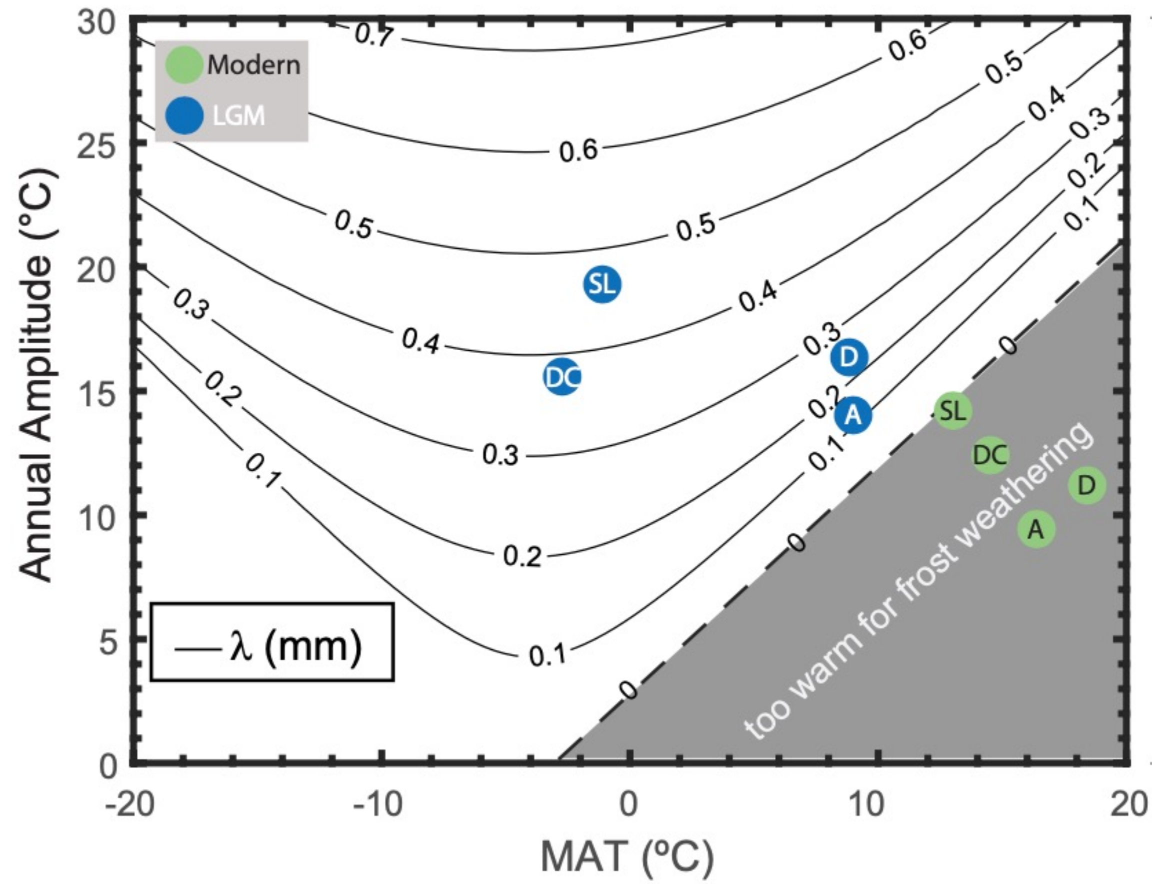

The legacy of damage in past climates may influence near-surface crack patterns accessed by water today.

Marshall et al., 2021

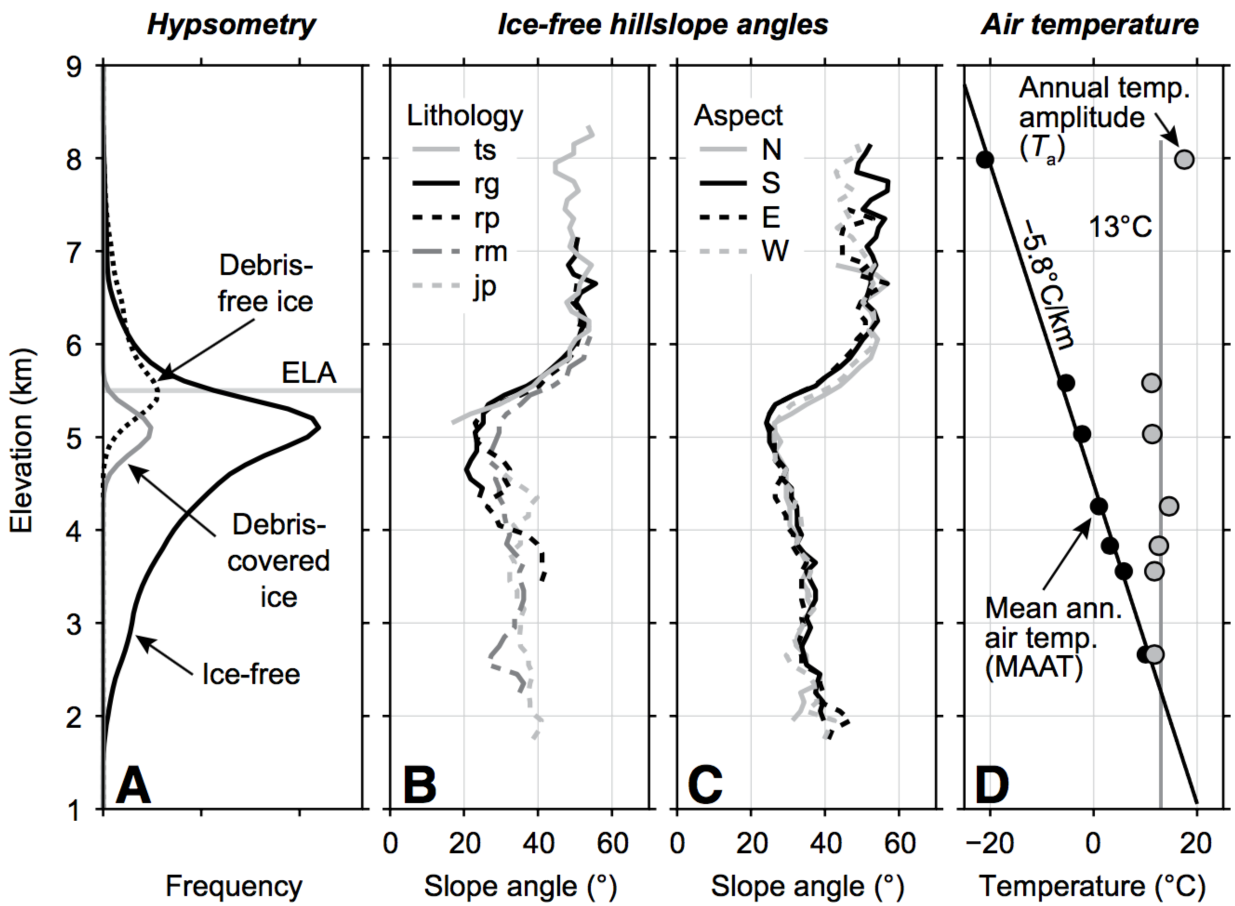

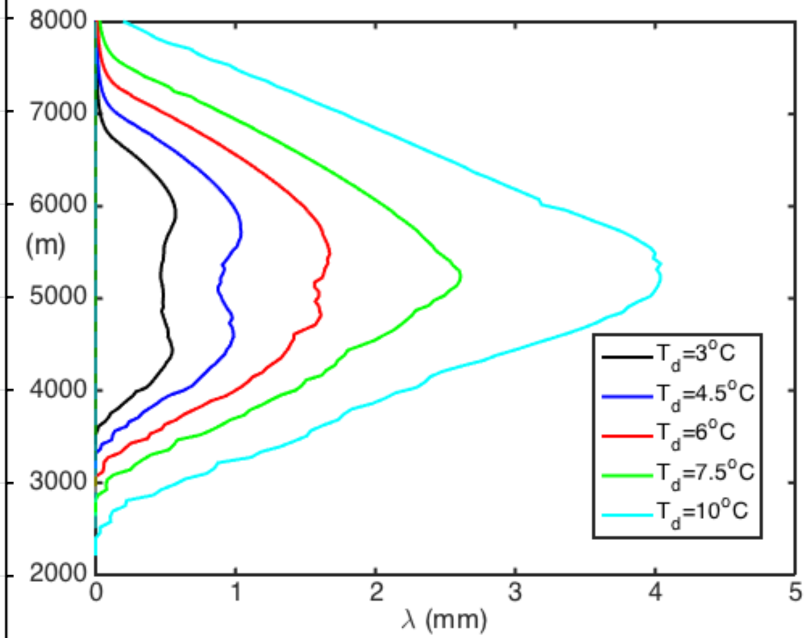

Scherler, 2013

Some evidence from landscape form for enhanced cracking at particular climatic thresholds.

Note: location of damage relative to pre-existing joints likely important.

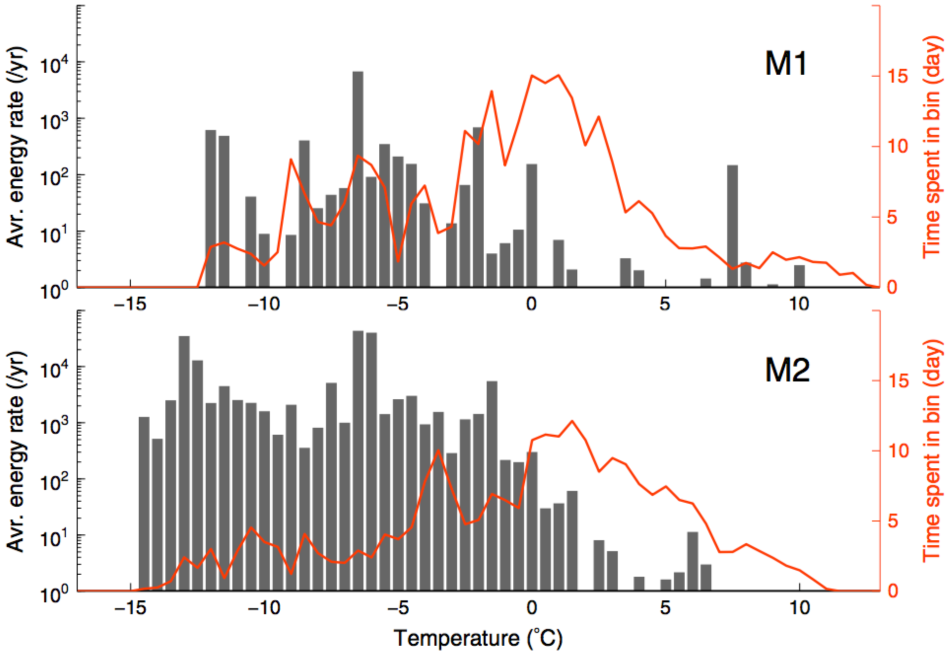

Girard et al., 2013

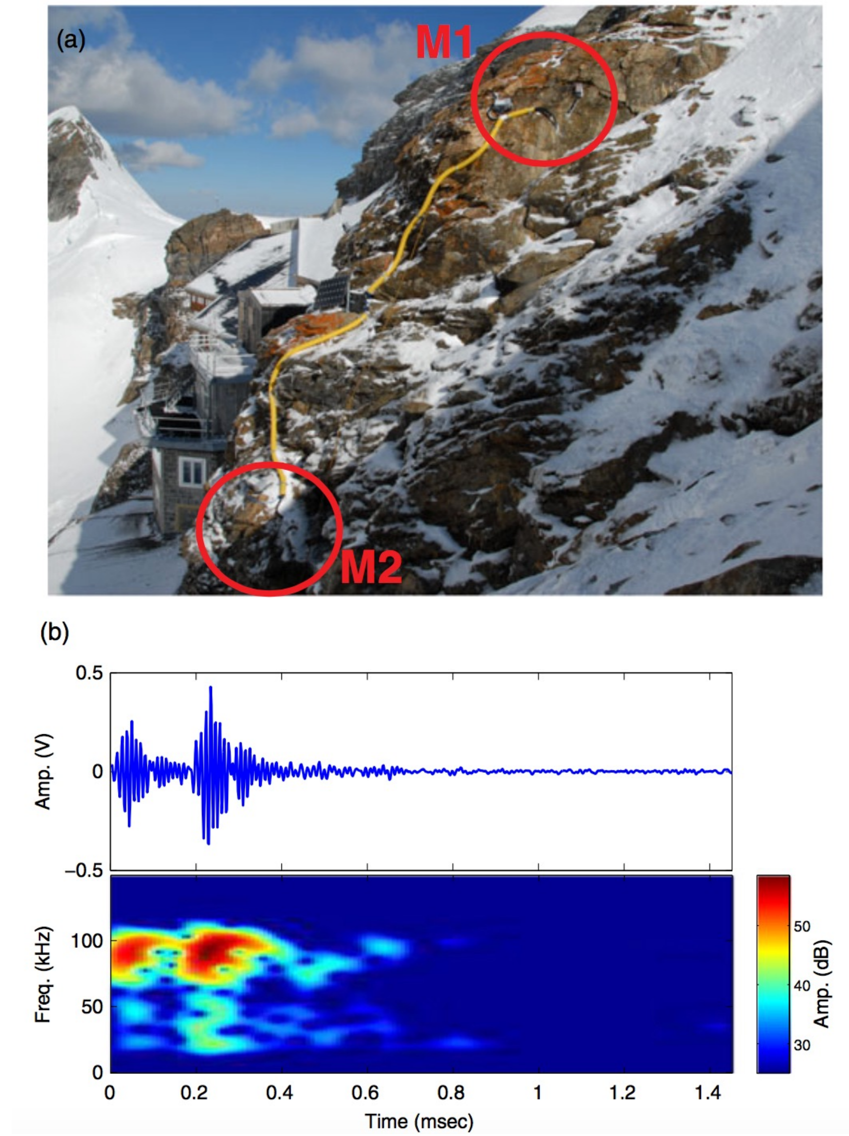

Other evidence of cracking doesn't appear to have the predicted low-temperature fall-off.

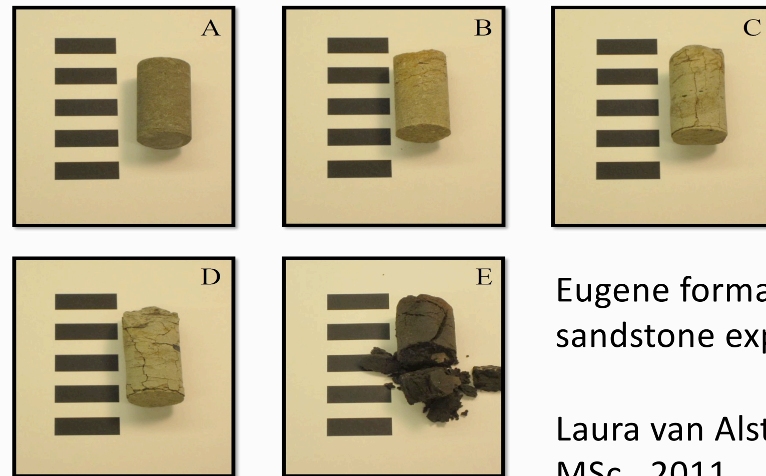

Eugene formation sandstone expts.

Laura van Alst, MSc., 2011

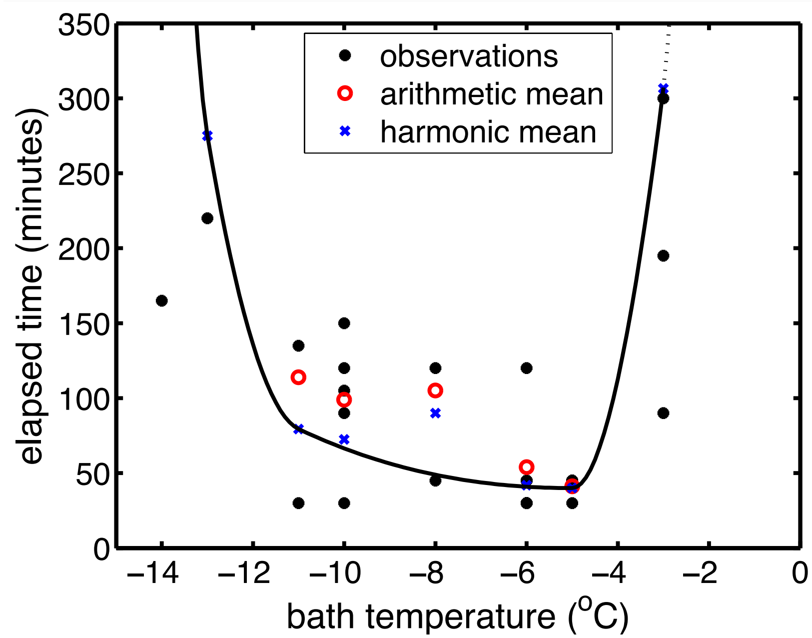

Procedure:

1. beaker-soak one-inch cores
2. wrap in plastic (avoid contact with glycol)
3. drop in glycol bath at fixed *T*
4. inspect frequently until cracks detected

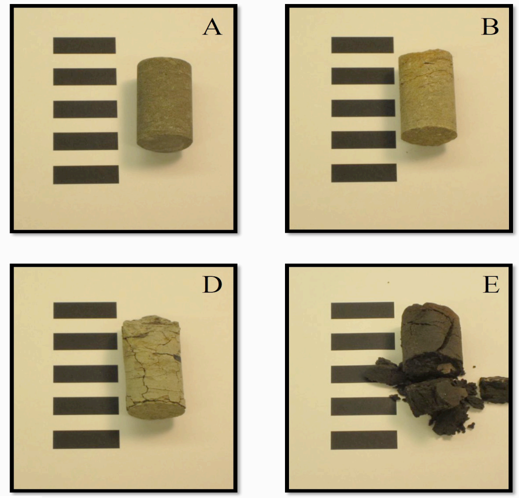

Eugene formation sandstone expts.

Laura van Alst, MSc., 2011

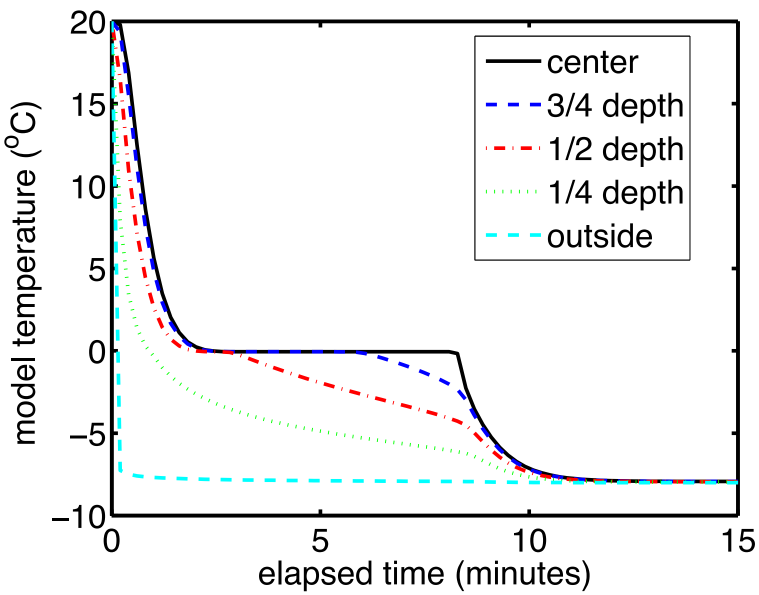

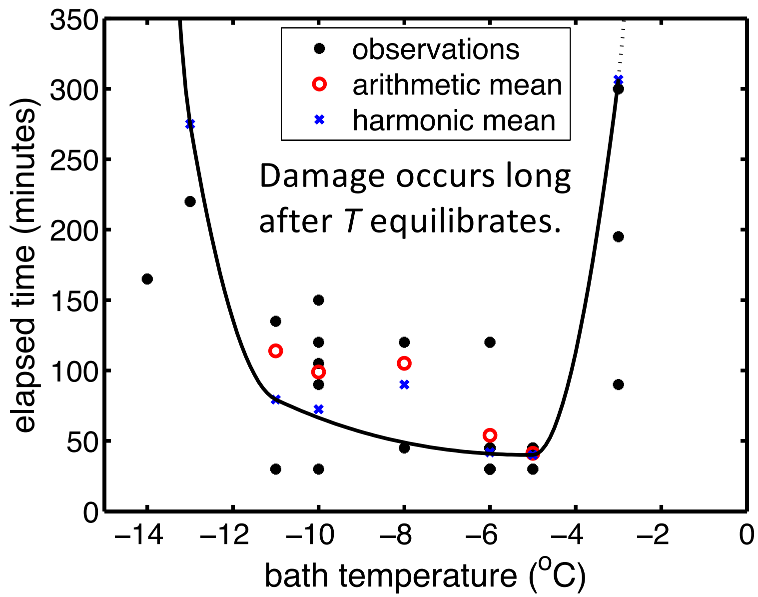

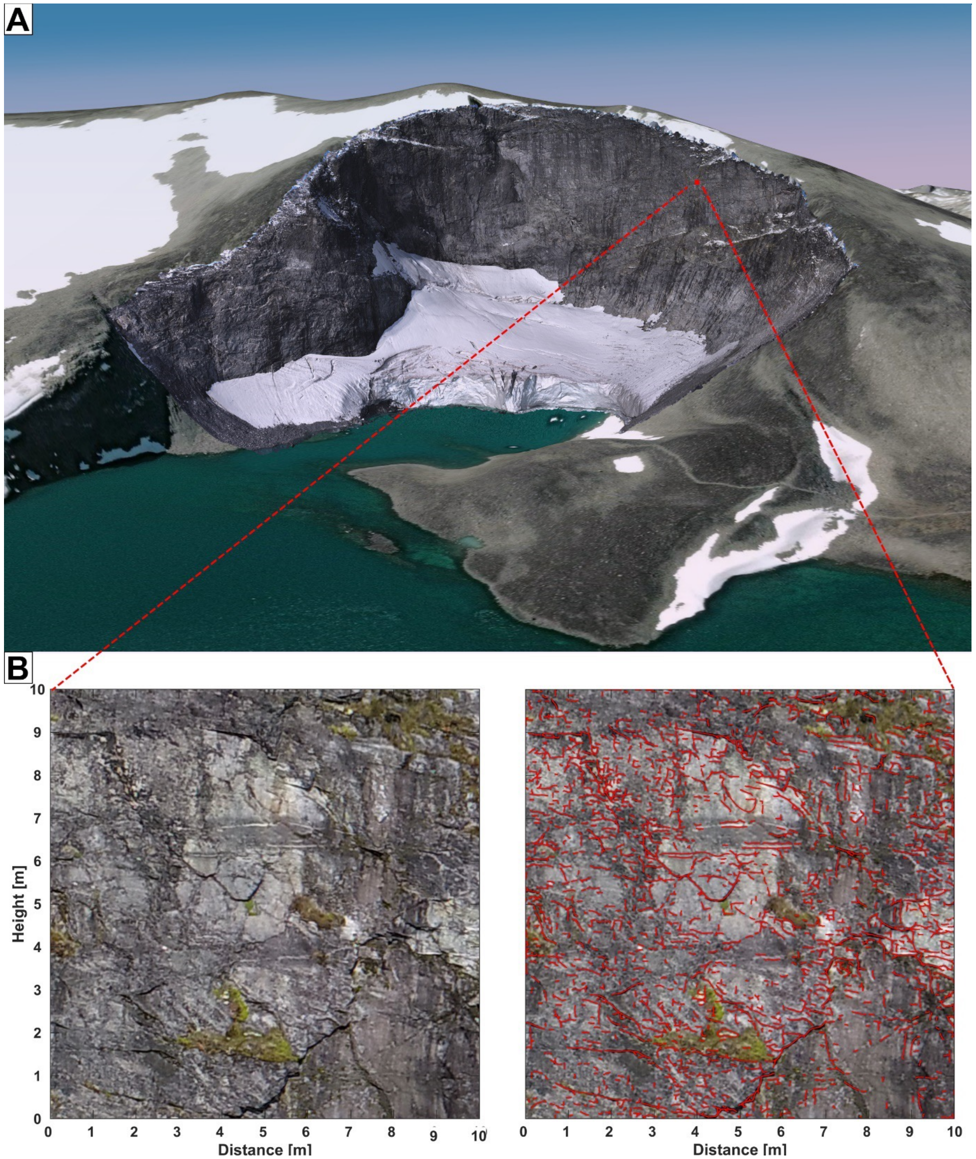

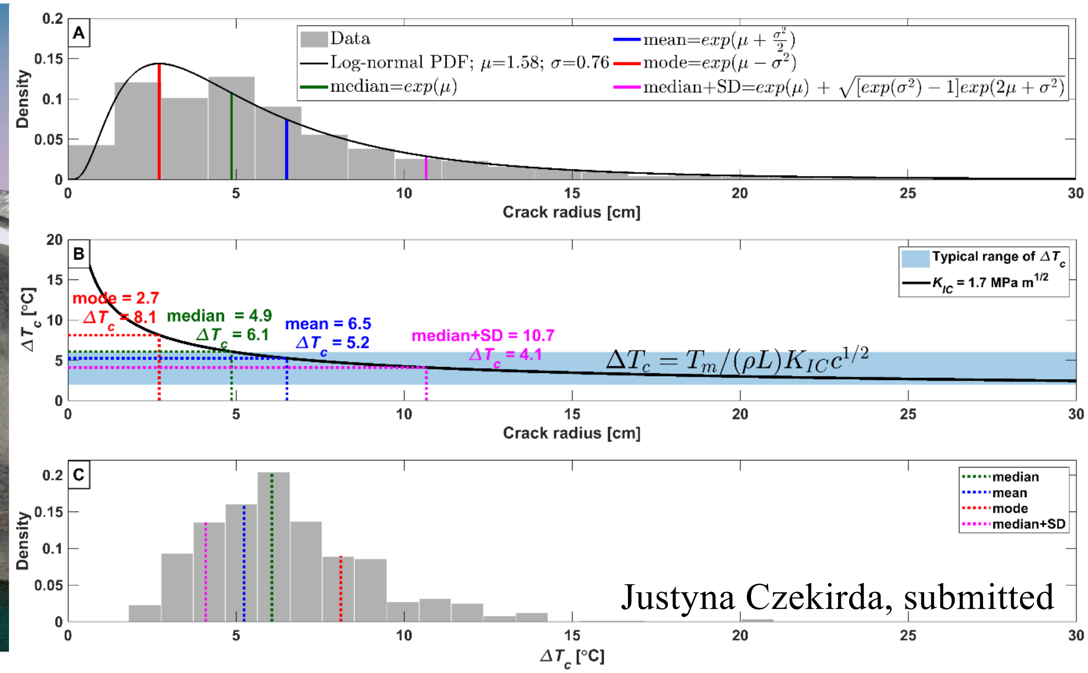

A single crack size is likely too idealized.

Evidence suggests coarsening with large cracks cannibalizing the ice formed initially in small cracks.

A statistical approach might be called for?

With unsaturated conditions the sizes of the largest saturated flaws should be reduced, increasing ΔT_{cu}.

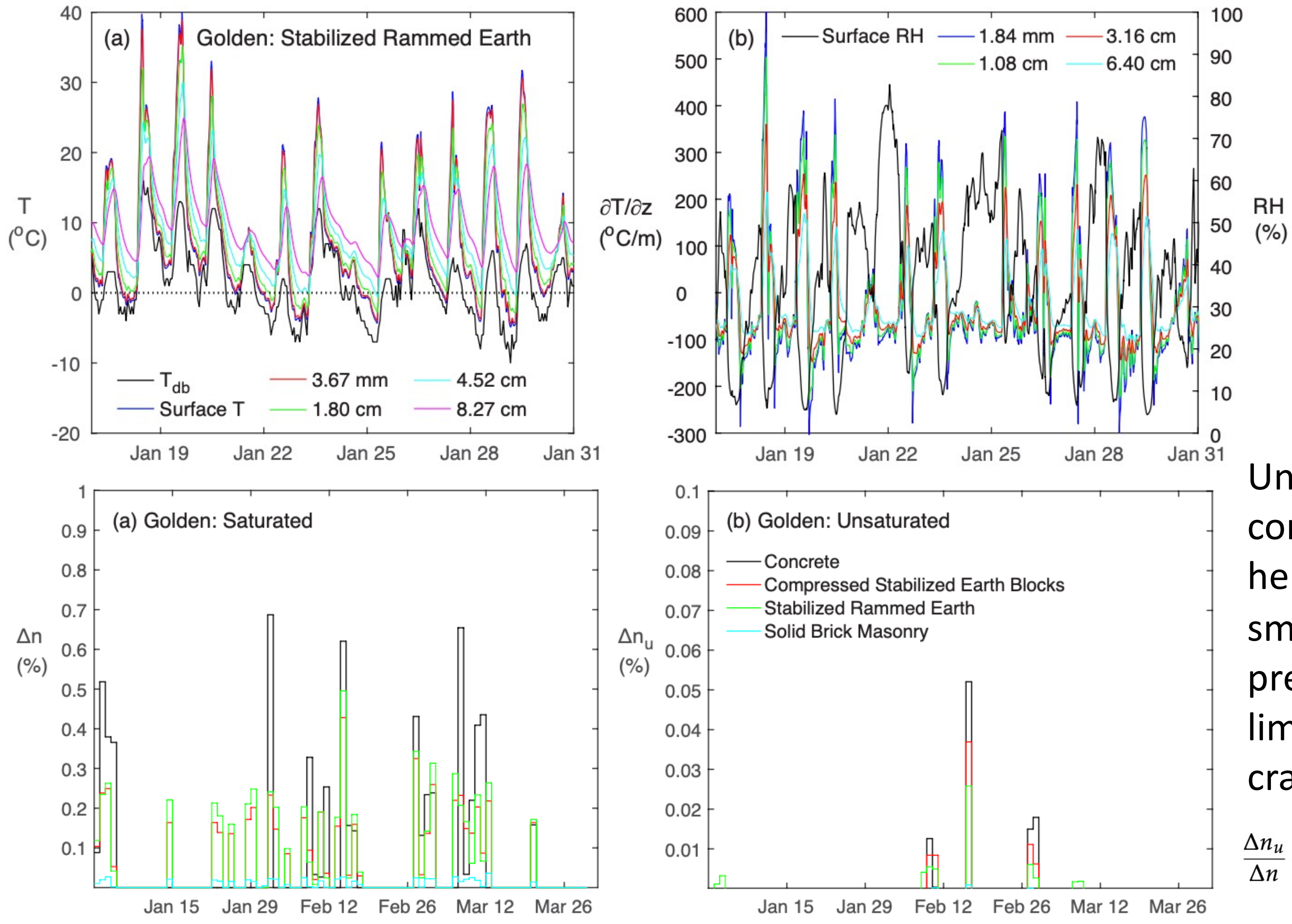

Unsaturated conditions treated here by assuming small pores filled preferentially, limiting characteristic crack size so that:

$$\frac{\Delta n_u}{\Delta n} \sim \left(\frac{T_m - T_c}{T_m - T_{cu}}\right)^{\alpha+1} \approx S^{(\alpha+1)/(2\beta)}$$

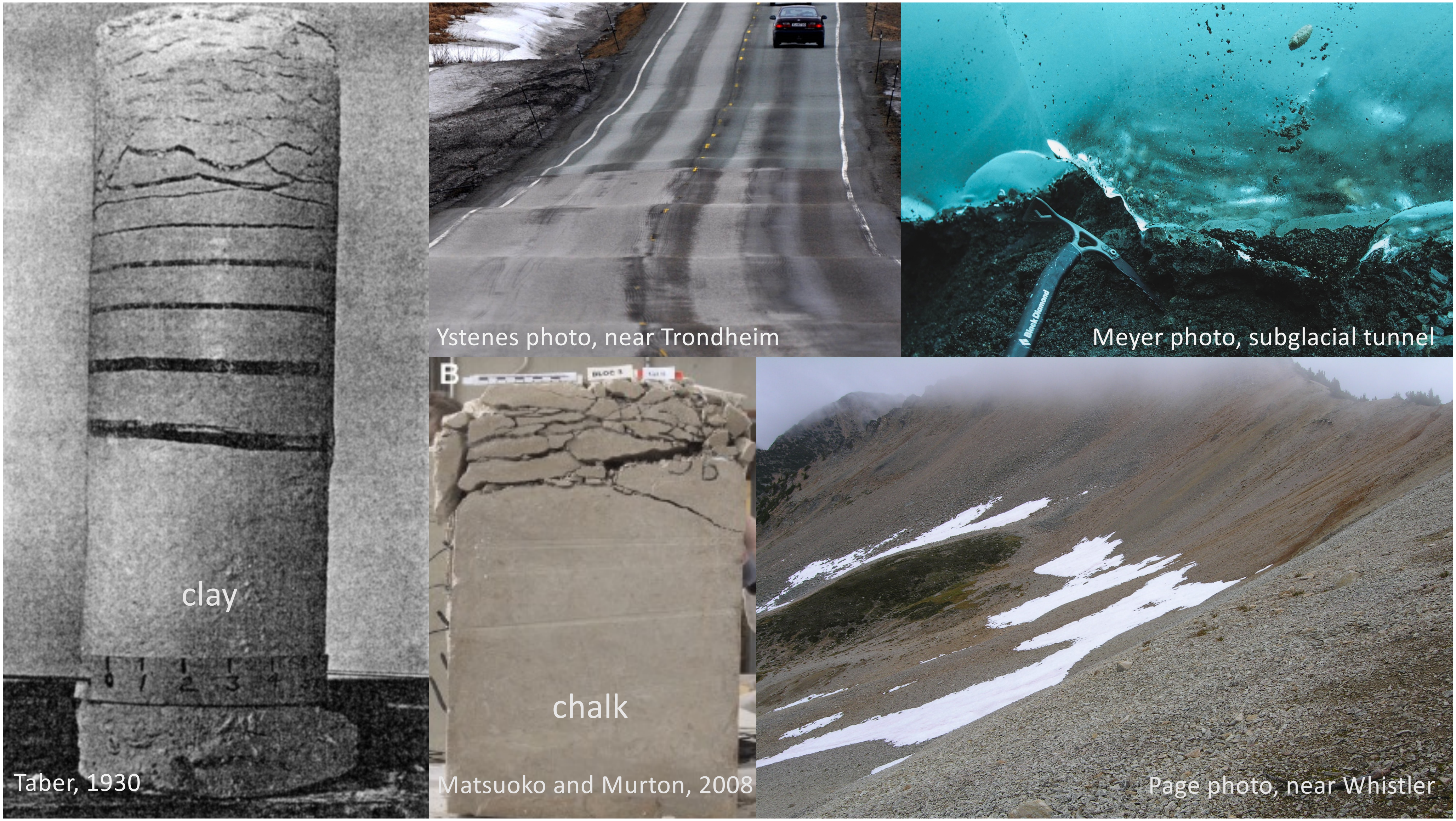
clay
Taber, 1930
Ystenes photo, near Trondheim
Meyer photo, subglacial tunnel
B
chalk
Matsuoko and Murton, 2008
Page photo, near Whistler

Sources (ordered by slide number of first appearance)

2 Taber, S. (1930). The mechanics of frost heaving. *The Journal of Geology*, *38*(4), 303-317.

Matsuoka, N., & Murton, J. (2008). Frost weathering: recent advances and future directions. *Permafrost and Periglacial Processes*, *19*(2), 195-210.

9 Hallet, B., Walder, J. S., & Stubbs, C. W. (1991). Weathering by segregation ice growth in microcracks at sustained subzero temperatures: Verification from an experimental study using acoustic emissions. Permafrost and Periglacial Processes, 2(4), 283-300.

10 Walder, J., & Hallet, B. (1985). A theoretical model of the fracture of rock during freezing. Geological Society of America Bulletin, 96(3), 336-346.

13 Vlahou, I., & Worster, M. G. (2015). Freeze fracturing of elastic porous media: a mathematical model. Proceedings of the Royal Society A: Mathematical, Physical and Engineering Sciences, 471(2175), 20140741.

15 Hales, T. C., & Roering, J. J. (2007). Climatic controls on frost cracking and implications for the evolution of bedrock landscapes. Journal of Geophysical Research: Earth Surface, 112(F2).

Anderson, R. S. (1998). Near-surface thermal profiles in alpine bedrock: Implications for the frost weathering of rock. Arctic and Alpine Research, 30(4), 362-372.

18 Anderson, R. S., Anderson, S. P., & Tucker, G. E. (2013). Rock damage and regolith transport by frost: An example of climate modulation of the geomorphology of the critical zone. Earth Surface Processes and Landforms, 38(3), 299-316.

20 Rempel, A. W., Marshall, J. A., & Roering, J. J. (2016). Modeling relative frost weathering rates at geomorphic scales. Earth and Planetary Science Letters, 453, 87-95.

24 Marshall, J. A., Roering, J. J., Rempel, A. W., Shafer, S. L., & Bartlein, P. J. (2021). Extensive frost weathering across unglaciated North America during the Last Glacial Maximum. Geophysical Research Letters, 48(5), e2020GL090305.

25 Scherler, D. (2014). Climatic limits to headwall retreat in the Khumbu Himalaya, eastern Nepal. Geology, 42(11), 1019-1022.

26 Girard, L., Gruber, S., Weber, S., & Beutel, J. (2013). Environmental controls of frost cracking revealed through in situ acoustic emission measurements in steep bedrock. Geophysical Research Letters, 40(9), 1748-1753.

27 Rempel, A. W., & Van Alst, L. J. (2013). Potential gradients produced by pore-space heterogeneities: application to isothermal frost damage and submarine hydrate anomalies. In Poromechanics V: Proceedings of the Fifth Biot Conference on Poromechanics (pp. 813-822).

Van Alst, L. J. (2011). Laboratory experiments in cold temperature rock deformation (MSc thesis, University of Oregon).

30 Rempel, A. W., & Rempel, A. R. (2019). Frost resilience of stabilized earth building materials. *Geosciences*, *9*(8), 328.